ACS APPLIED NANO MATERIALS

UNIVERSITY OF EXETER

Subscriber access provided by the University of Exeter

Review

Graphene Foams for Electromagnetic Interference Shielding: A Review

Zhenxin Jia, Mingfa Zhang, Bin Liu, Fucheng Wang, Gang Wei, and Zhiqiang Su

ACS Appl. Nano Mater., **Just Accepted Manuscript** • DOI: 10.1021/acsanm.0c00835 • Publication Date (Web): 24 Jun 2020

is published by the American Chemical Society. 1155 Sixteenth Street N.W., Washington, DC 20036

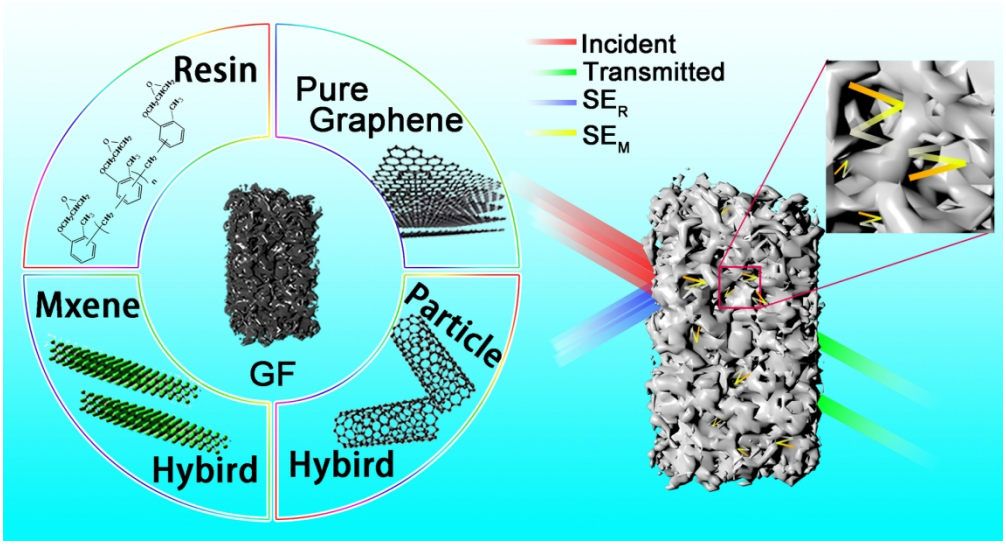

TOC

82x44mm (600 x 600 DPI)

Graphene Foams for Electromagnetic Interference Shielding: A Review

*Zhenxin Jia,[‡a] Mingfa Zhang,[‡b] Bin Liu,[c] Fucheng Wang,[d] Gang Wei[*c] and Zhiqiang Su[*a]*

[a] *State Key Laboratory of Chemical Resource Engineering, Beijing University of Chemical Technology, 100029 Beijing, China.*

[b] *Laboratoire de Tribologie et Dynamique des Systèmes (LTDS), École Centrale Lyon, Écully, France.*

[c] *College of Chemistry and Chemical Engineering, Qingdao University, 266071 Qingdao, China*

[d] *Zhejiang University of Technology, Hangzhou, China.*

‡These authors contributed equally

Abstract: Electromagnetic shielding materials generated with the extensive application of electromagnetic wave have been utilized in military radar stealth, electromagnetic shielding of advanced electronic equipment, electromagnetic radiation protection, and other fields. With the quick development of internet and electronic devices, a large number of electromagnetic waves flood into the living environment, affecting human life and health potentially. Meanwhile, further development and applications of terahertz(THz) electromagnetic detection technology challenge the research of electromagnetic interference shielding (EMIS). Therefore, EMIS materials have been developed towards the direction of high efficiency, wide bandwidth, and lightweight. However, traditional single metal-based and polymer-based EMIS materials cannot meet the demand. Current studies confirmed that graphene, especially graphene foam (GF)-based EMIS materials, has become one of the most potential EMIS materials in the field of electromagnetic wave loss and absorption due to its unique physical structure, excellent electrical and mechanical properties. GF, a three-dimensional (3D) graphene structure prepared from graphene and its derivatives, not only fully utilizes to the unique physical and chemical properties of graphene, but also further reduces the density of EMIS materials and improves

the EMIS performance. This work expounds the potential value of graphene in the field of EMIS based on the mechanism of EMIS, then summarizes the recent progress of GF-based materials for EMIS applications. More focus on the effects of different preparation methods towards the structure, mechanical properties, and EMIS performance of GF materials are introduced and discussed in detail.

KEYWORDS: graphene foams, ultralight, wideband, terahertz wave, three-dimensional structure, electromagnetic shielding.

1. Introduction

In recent years electronic information technology develops rapidly, and various electronic equipment have been extensively applied in engineering, civil, aerospace, military, and other fields.[1-2] Currently, humans are more dependent on electronics than ever before, and electronic devices bring great convenience to our life.[3-4] While bringing convenience to human beings, electronic devices have also brought potential harm and effects. Due to the intensive use and spread of electronic equipment, the space is filled with electromagnetic waves of different wavelengths and frequencies, and a large amount of which has a great impact on the survival and development of human beings.[5] On the hand, the rapid development of modern high-technology has made human society put forward higher requirements for the accuracy of electronic equipment. However, during the operation of electronic equipment, electromagnetic radiation will be generated continuously and radiated outward. Mutual radiation between electronic elements seriously affects the working accuracy of electronic devices and restricts the development of electronic industry.[6-8] On the other hand, since current electronic communication uses electromagnetic waves as a carrier, the electromagnetic interference (EMI) is very likely to cause channel instability, which affect the quality, cause important information leakage, and even endanger commercial and national security.[9-11]

Most importantly, modern medicine has proved that long-term electromagnetic radiation affects the health of the human body. The electromagnetic radiation energy could be transmitted to cells, resulting in abnormal body temperature and protein inactivation. In addition, the electromagnetic wave increased the possibility of gene mutation, increasing the incidence of teratoma and cancers.[1, 12-14] Besides the above-mentioned shortcomings, the pollution of air and

water caused by the electromagnetic effects have become the fourth major hazard to human survival and safety (**Figure 1a.**). Therefore, the research and development of electromagnetic interference shielding (EMIS) materials with high efficiency and wide bandwidth are extremely urgent.[15-16] Over the past years, the new generation detection technology-terahertz (THz), refers to electromagnetic waves with a wavelength of 30 um to 3 mm, has been widely valued (**Figure 1b.**), attracting great interest due to its excellent performance such as broadband, transient, high permeability, and fingerprint spectrum.[17-18] However, the development of EMIS materials in THz band is relatively backward, and there are only a few materials that can effectively shield THz electromagnetic waves,[19-22] which bring the urgent requirement for the design and fabrication of new generation of EMIS materials.

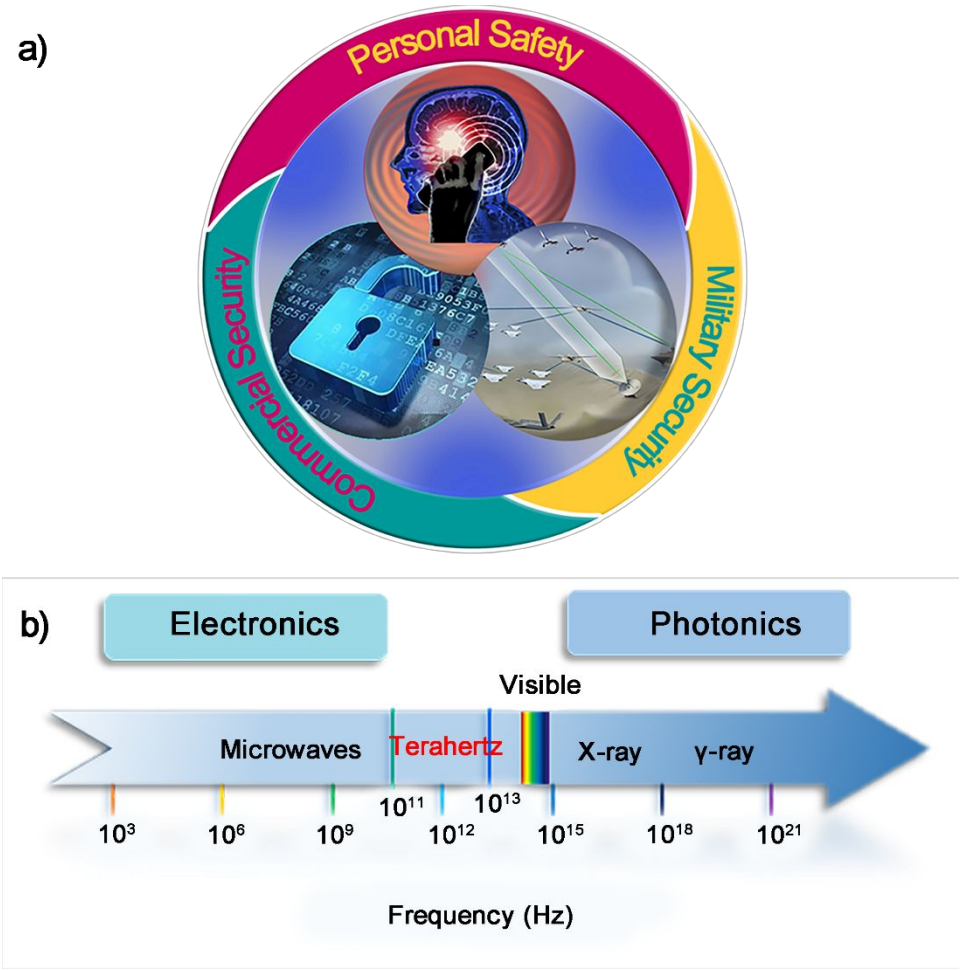

Figure 1. a) The harm of electromagnetic wave, and b) The location of THz in electromagnetic spectrum.

In the past few decades, limited by science and technology, metal- and polymer-based EMIS materials have been mainly studied.[23-24] Metal materials have higher electric conductivity, and the magnetic metal materials also have high magnetic permeability, and therefore the metal-based EMIS materials had wider bandwidth and higher shielding effect than other EMIS materials.[25-26] However, metal-based EMIS materials are dense and corrosive, which limits their further development.[10] Compared with metal materials, polymer-based EMIS materials are corrosion resistant, light, easy to process and adjustable,[27-28] but their electrical conductivity is not satisfactory. Therefore, more efforts have been performed to improve their conductivity by adding conductive fillers such as graphite, carbon black, and metal particles.[29] However, this approach is severely limited due to the agglomeration of fillers. Until now, the performance of EMIS materials is far from the expected higher shielding efficiency, wider absorption bandwidth, lighter mass and better mechanical properties.[30-31]

Graphene, the popular two-dimensional (2D) material discovered in the world, has been the research hot spot since its discovery.[3, 31-32] Graphene has great potential in the field of EMIS due to its excellent charge-transfer properties, large specific surface area and excellent mechanical properties.[15, 33-35] It has been found that the graphene-based EMIS materials meet the needs of EMIS with the properties of "broadband", "light", and "high strength". In the graphene-based EMIs, researchers often choose graphene as a filler to enhance the EMI of the materials. Due to the poor dispersion of graphene, the inability to form a continuous conductor and the low structural strength, the development of graphene electromagnetic shielding materials was limited. 3D graphene has a long-range consecutive interconnection network, which enhances the electrical conductivity of the material. Compared with 2D graphene materials, 3D graphene has higher EMIS efficiency In addition, in 3d graphene, the stacking and folding of graphene sheet layers and the pore structure of 3d graphene can enhance the reflective area of the material, increase the multiple reflection losses of the material, and further improve the electromagnetic shielding efficiency of the material. Moreover, the ultra-high porosity of the graphene foam can reduce the density of the material. [36-38]

Herein, we present the development of graphene foam (GF)-based materials for EMIS application in recent years through discussing the EMIS mechanisms, the fabrication of GF-based EMIS materials, and the influence of graphene microstructure and GF structure on the EMIS

performance. It is expected that this paper can provide help for the design and fabrication of GF electromagnetic shielding materials.[39-40]

2. EMIS Mechanisms

When electromagnetic waves are transmitted to the surface of an electromagnetic shield, they first interact with the surface and then reflect off the surface of materials, resulting in a reflection loss (SE_R).[41-42] Those waves that are not lost by reflection penetrate the surface of materials and enter the interior of the material body, part of which is absorbed by the material body forming absorption loss (SE_A). When the electromagnetic wave in the shielding materials propagates to another interface, it is reflected again and dissipates energy in the shielding body, forming multiple reflection loss (SE_M),[43-45] as shown in **Figure 2.** The evaluation index of EMIS performance of materials is defined as SE,[41, 46] and The total effectiveness (SE_T) of EMI is the sum of the above three shielding effect, expressed as $SE_T=SE_R+SE_A+SE_M$.

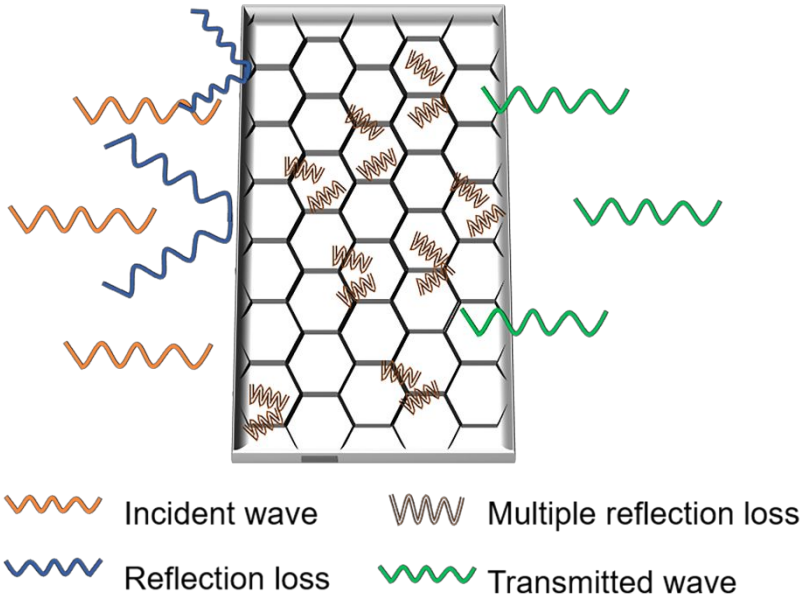

Figure 2. Schematic diagram of EMIS mechanism.

The SE_T, SE_R and SE_A of materials are determined by the following expressions，

$$SE_T = -10\lg(|S_{12}|^2) = -10\lg(|S_{21}|^2).$$

$$SE_R = -10\lg(1-|S_{11}|^2).$$

$$SE_A = -10\lg\left(|S_{21}|^2/(1-|S_{11}|^2)\right).$$

where, S_{11}, S_{22} are the reflection coefficients and S_{12}, S_{21} are the absorption coefficients.

Due to the different inherent impedance between the space and the shielding materials, the alternating electromagnetic field of electromagnetic wave interacts with the conductive particles on the surface of the shielding material, resulting in SE_R on the surface of the designed material.[44, 47] The formula can be expressed as:

$$SE_R = 168 - 10\lg\left(fu_r / \sigma_r\right).$$

Obviously, the SE_R of material is mainly affected by the electromagnetic wave frequency f, the permeability of materials to copper (μ_r), and the relative conductivity of materials to copper (σ_r). Therefore, at a fixed frequency, the smaller the μ_r/σ_r ratio, the larger the SE_R, which means that increasing the conductivity or decreasing the permeability of the shielding material can increase the value SE_R.

When electromagnetic waves penetrate a material surface and enter the interior of shielding bodies, both electric and magnetic dipoles in the material are affected by the interaction of alternating electromagnetic fields and generate oscillation, which causes the energy of electromagnetic wave to be converted into the mechanical energy of the dipole vibration, thereby reducing the electromagnetic wave energy and forming SE_A. Since the electromagnetic wave at this time penetrates the material surface and enters into the interior of a material, the value of SE_A is related to the thickness, conductivity, permeability, and natural frequency of the shielding material.[48-49] The formula is as follows:

$$SE_A = 1.314d(fu_r\sigma_r)^{1/2}$$

From this equation it can be seen that the material with relatively high electrical conductivity and magnetic permeability will have better SE_A performance. In addition, the SE_A of the material is also affected by the thickness (d) of the material, showing a linear correlation. Electromagnetic waves penetrate the surface of the shielding material and continue to propagate in the material body. When they propagate through the material to the other side of the surface, the electromagnetic wave will reflect or penetrate the material.[48, 50] The reflected electromagnetic waves will further attenuate in the material body and cause multiple reflection and loss, thus forming SE_M, which is expressed as follows: $SE_M = 20\lg\left(1 - e^{-2d/\delta}\right)$. Here, δ represents the thickness of the material through which the electromagnetic wave penetrates, that is, the skin depth. There are a lot of phase interfaces inside the 3D graphene, where electromagnetic waves

are constantly reflected and lost, making the GF have a very considerable performance of multiple reflection loss.

3. Graphene for EMIS

Carbon-based EMIS materials, such as carbon nanotubes (CNTs), carbon black, graphite, carbon fibers, and silicon carbide fibers have been studied for a long time, but it was found that these materials have relatively high density, easy oxidation, and other inevitable shortcomings.[3, 5] The new EMIS materials always pursue the characteristics of "lighter, wider and stronger". As ideal quasi one-dimensional (1D) carbon nanomaterials, CNTs are one of the alternative candidates for the fabrication of novel EMIS materials.[51] However, their high capacitance and low permeability restrain their development in the field of EMIS.

Compared with existing carbon materials, graphene reveals higher electrical conductivity, larger specific surface area, and higher chemical stability, is one of the optimal materials for EMIS.[52] Most importantly, the 3D network structure prepared from graphene has a continuous conductive skeleton, which gives the fabricated materials higher conductivity. In addition, the porous structure increases the electromagnetic wave reflection surface, thus further improving the EMIS performance of materials. On the other hand, the excellent mechanical strength and chemical stability of graphene broaden the practical applications of EMIS materials.[6, 53-54]

3.1. Graphene Microstructure for EMIS

Graphene is a perfect honeycomb crystal formed by a single layer of carbon atoms and has a 2D structure.[55] The unique electronic structure of graphene endows graphene with ultra-high conductivity, which enables graphene-based EMIS materials to achieve excellent SE_A. The SE_R and SE_A of EMIS can be adjusted by introducing defects in reduced graphene oxide (rGO). The perfect honeycomb crystal structure enables graphene-based EMIS materials to achieve higher physicochemical stability.[52, 56-58]

The π bonds outside the graphene layer give graphene electronic conductivity and result in weak interactions between the graphene layers. Since there are two equivalent carbon sub-grids in the honeycomb crystal, the conical valence band and conduction band intersect at K and K‘ in the Brillouin zone at the Fermi energy level,[59-61] as shown in **Figure** 3. The perfect graphene

honeycomb lattice allows electrons to pass through smoothly, and the electron or hole concentration is as high as 1013 cm^{-2}, showing extremely high carrier mobility (approximately 500000 $cm^2/(V \cdot s)$). According to the EMIS mechanism, graphene materials with extremely high electrical conductivity can greatly improve the $\mu_r\sigma_r$ value at a fixed frequency, thus increasing the SE_A efficiency of the shielding body effectively.[33, 62-64]

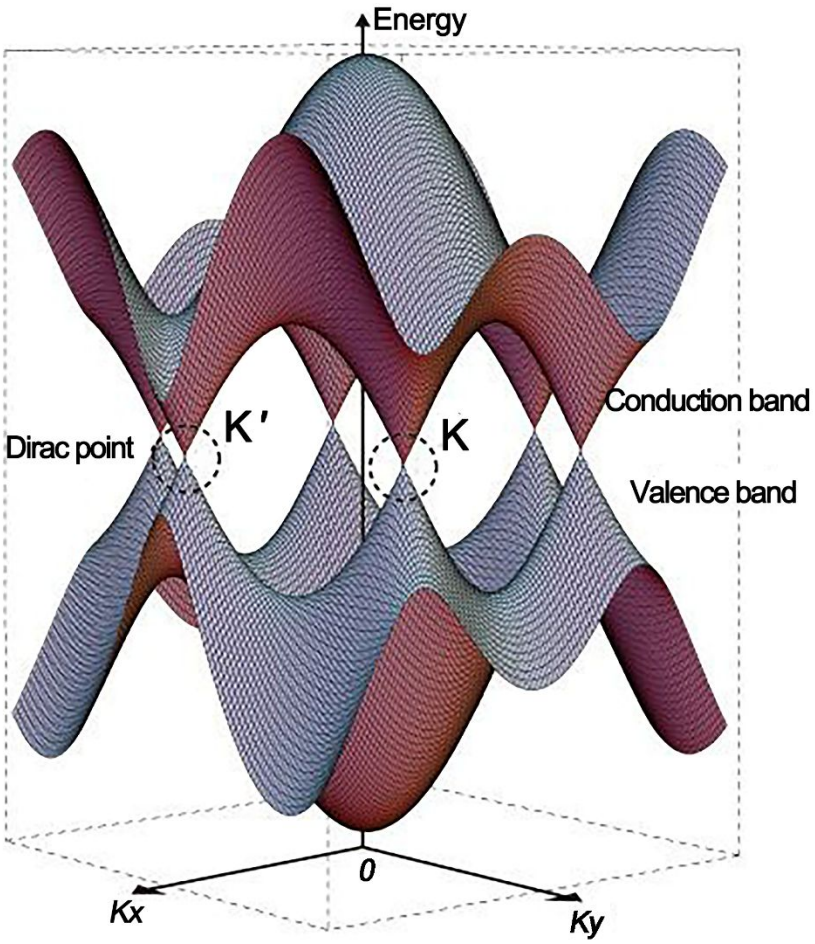

Figure 3. Energy bands near the Fermi level in graphene. The conduction and valence bands cross at points K and K′ nm (reproduced with permission from ref. [59], Copyright 2009 Nature Publishing Group).

Since the excellent electrical conductivity of graphene reduce the μ_r/σ_r ratio, the reduced compatibility of graphene with the space impedance results in a high SE_R of the prepared EMIS materials. However, high SE_R in some fields is not in line with the requirements for applications.[65] Graphene based EMIS prepared from GO as the main raw material can improve the problem of "high reflection" and "low absorption" of graphene materials. This is due to a

large amount of oxygen-containing functional groups in GO, which improves the impedance matching characteristics of the materials.[66]

Although the sizeable conjugated system makes it a negatively charged system, it is possible to react with electrophiles. However, it is worth noting that graphene has few reactive sites and therefore has more stable chemical properties. On the other hand, the mechanical properties of graphene are fantastic due to its special structure. Therefore, compared with traditional EMIS materials, graphene-based EMIS materials would gain a broader range of applications.[6, 67-68]

3.2. GF Structure for EMIS

Assembling graphene sheets into GF can not only exert the characteristics of graphene but also enhance the EMIS of the material through structural control. Previously, it has been reported the interconnected network GF structure can be fabricated by the hydrothermal reaction, template synthesis, self-assembly, sol-gel synthesis, and other techniques. Furthermore, the formation of porous structures can further reduce the overall density of graphene-based materials and meet the development requirements of lightweight applications such as satellites, space stations, unmanned aerial vehicles, commercial aircraft and so on.[69] In addition, graphene is the primary raw material for preparing GF structure. The stacking and folding of graphene sheets increase the SE_A of the electromagnetic waves, and the continuous interconnect network structure between graphene sheets can form a larger conductive network, which increases the EMIS efficiency of the designed materials.[70] Besides, due to the large number of porous structures inside the pore, the electromagnetic waves can keep SE_M in the pore. Finally, it should be noted that lightweight, porous GFs can be adjusted and controlled effectively for improving the EMIS performance through simple physical pressing.[71]

4. Fabrication of GF Structure for EMIS Applications

GF-based EMIS materials utilize noncovalent interactions such as the van der Waals force, π-π interaction, and electrostatic interaction to assemble or deposit a 3D network structure.[61, 63, 72] Previously, a lot of studies have been carried out in-depth to prepare GF-based EMIS materials through developing the fabrication strategies.[67] The properties of GFs including the 3D structure, mechanical strength, electrical conductivity, and EMIS effectiveness of materials are highly

related to the preparation methods of GFs.[73-75] At present, the main approaches for preparing GF-based EMIS materials include self-assembly,[76] template method,[77] and sol-gel method.[78-79]

4.1. Self-assembly Synthesis of GFs for EMIS

4.1.1. Pure GFs for EMIS

The self-assembly method, also known as solvothermal method, refers to the formation of GF with macropores and mesopores structures by gathering graphene sheets and stacking them to form physical cross-linking points under the π-π interaction. The preparation process consists primarily of treating the sealed container containing the GO suspension in a high-temperature environment for several hours, and then freeze-drying and annealing to obtain rGO foams,[80] the preparation operation is shown in **Figure 4a.** The solvothermal synthesis method is the most commonly used approach for preparing GF because of its simple process, easy control of reaction conditions, high purity and porosity of the product, and the ability to perform stoichiometric reactions. It is worth noting that since the self-assembly method uses GO as raw material, the graphene derivative rich in oxygen-containing functional groups has a high degree of impedance matching with the space environment. Electromagnetic waves are more easily penetrated into the shield body through the surface of the shield. Therefore, the SE_R of electromagnetic waves is small. This property makes the graphene-based foam EMIS material widely used in the fields of electromagnetic stealth, microwave absorption and the like.

The self-assembly method was first proposed by Shi *et al*. in 2010 for preparing GF.[81] Their team used GO as a precursor, and layers of GO were stacked on each other to successfully prepare interconnected 3D structures of graphene with electrical conductivity of 5× 10-3 s cm^{-1}. However, due to the collapse of interconnected network structures or the loss of hydrogen bond caused by drying and dehydrating during preparation, the prepared GF was too loose and its mechanical strength was not satisfactory. On the other hand, the structure of GF depends to some extent on the dispersion of the precursor. Wu *et al*. reported the preparation of GF with ultra-low density and high compression ratio by a solvent-thermal method.[82] This team explored the current hydrothermal method by using ethanol as the dispersed phase in the solvent thermal reaction. The dispersion solution was placed in a reactor at 180 ℃ for solvent thermal reduction to obtain the intermediate phase solid with a specific strength. After freeze-drying, annealing and other processes, the GF with high elasticity was finally obtained. By changing the dispersed phase, the

mechanical strength of the GF was increased and the compressible 3D GF structure with almost zero Poisson's ratio was prepared. This compressible 3D graphene structure can realize the controllable shielding of electromagnetic waves, which has important application value in the field of intelligent materials. It can appropriately adjust the electromagnetic shielding efficiency according to the changes in the environment. Shen explores to improve GO reduction and obtains ultra thin GF with high electromagnetic shielding effectiveness (~25.2dB, 0.3mm)[83].The solution they adopted was to add reducing agent in the process of GO hydrothermal reduction. GF with higher reduction degree can be obtained by hydrothermal reduction and chemical reduction.In addition, GF obtained by this method has a significant network structure, which increases the energy loss of electromagnetic wave in the material body.

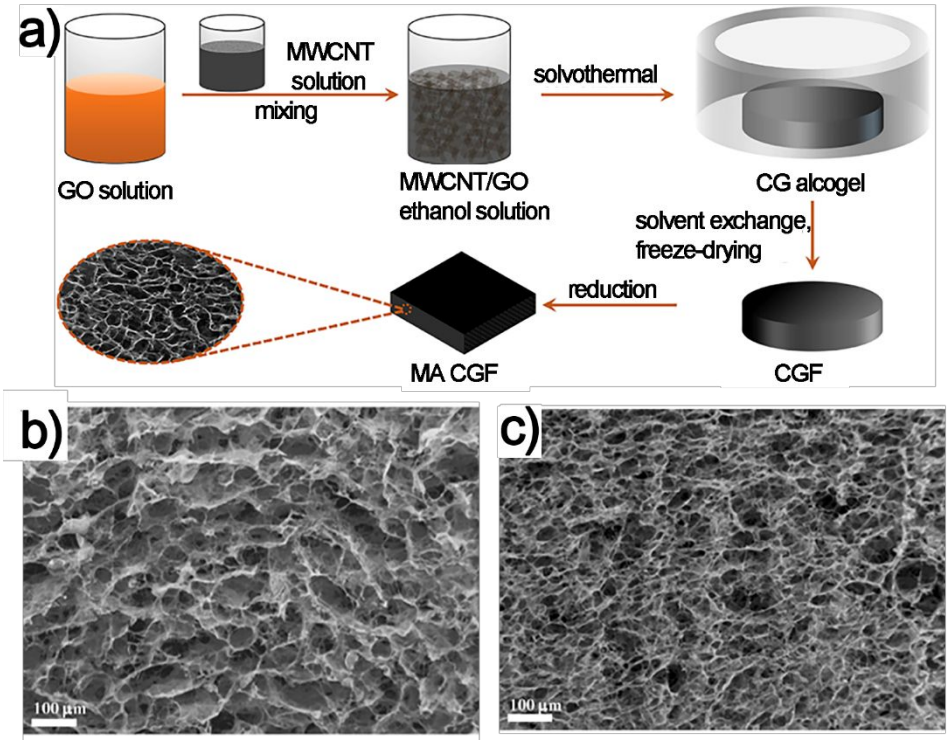

Figure 4. a) Schematic illustration of the fabrication process of MA CGF (a reproduced with permission from ref. [80], Copyright 2017, Elsevier). The cross-sectional SEM images of C0.6 (b) C0.9 (c) powders, (c reproduced with permission from ref. [84], Copyright 2016, Elsevier).

Huang *et al*. further explored the regulation of the chemical composition and physical structure of GF by adjusting the concentration of GO dispersion and the temperature in the

thermal reduction process.[84] Experimental results show that the increase of the concentration of the original dispersion possess more restacking structures, as shown in **Figure 4b and c**. Pozuelo et al. investigated the effect of heat treatment temperature on GO reduction degree[85]. They first obtained the rGO aerogel by hydrothermal synthesis. Then, the rGO aerogel was heat-treated at 400 ℃, 600 ℃ and 1000 ℃.The effects of different temperature on rGO reduction degree and structure of rGO aerogel were analyzed. It is found that the increase of heat treatment temperature can remove the oxygen-containing functional groups on the GO sheet layer, making the spacing of rGO sheets gradually decrease. However, the increase of annealing temperature did not have a great influence on the spatial structure of rGO aerogels. Thanks to fewer defects of rGO lamella, rGO aerogel has higher electric conductivity, which makes the rGO aerogel has higher reflection loss efficiency, in addition, the high annealing temperature remains space mesh structure can make rGO aerogel has high absorption efficiency loss and multiple reflection loss efficiency, so as to promote the material of electromagnetic shielding effectiveness (~ 40 dB, 5 mm).

4.1.2. GF Based Composite

Although the strength of 3D graphene has been improved by changing the preparation process, it still cannot meet the strength requirement in some applications. More and more studies have been made to combine graphene and other materials to enhance the mechanical strength of GFs.

For instance, Chen *et al*. tried to enhance the 3D network structure of GF with phenolic resin and its pyrolysis derivatives.[86] The bending strength and bending modulus of aerogel increased by 67% and 20.2%, respectively due to the introduction of phenolic resin and its pyrolysis derivative amorphous carbon. This high strength and light weight electromagnetic shielding material can meet the requirements of more application scenarios, such as shielding room, supercomputer, base station and other fields. The EMIS performance of composite materials (shielding effect values of 25 dB (1 mm thick) and 33 dB (2 mm thick)) was closer or even exceed to that of GF prepared by chemical vapor deposition (CVD) method (~20 dB for 1 mm and <28 dB for 2 mm in the X-band range). Zhao *et al*. reported the successful synthesis of porous $Ti_3C_2T_x$/graphene foam with high conductivity by a hydrothermal method combined with the directional freezing method.[87] The significant improvement of this method is to reduce the reduction process of rGO at high temperature and simplify the preparation process of rGO foam.

In addition, the materials prepared by directional freezing have the structure characteristics of anisotropy, which gives the EMIS efficiency of the anisotropy of the materials. They proposed that GO sheets, which have a robust self-gelling ability, first form a 3D network structure during reduction. Under the polar interaction, $Ti_3C_2T_x$ was adsorbed to the outer surface of the graphene skeleton to realize the continuous construction of $Ti_3C_2T_x$/rGO shell and core structure, as shown in **Figure 5a.** Admirably, $Ti_3C_2T_x$ hybrid graphene composite foam exhibits an unimaginable conductivity of 1085 s/m due to its good structure and tight connection between the holes, and the EMIS efficiency of the material at a low load (0.74 vol %) reached 56.4 dB (2 mm), which is far beyond the qualified level, as shown in **Figure 5b**.

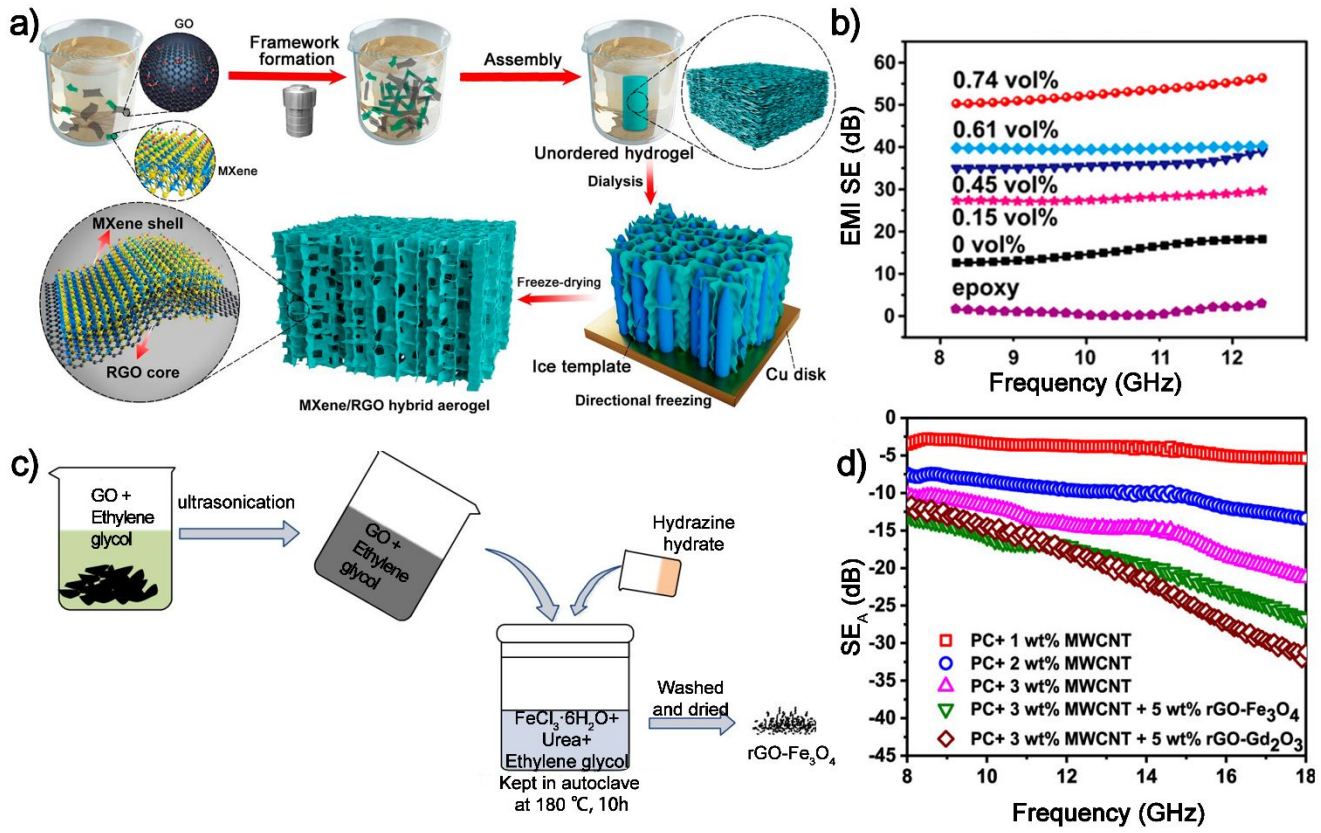

Figure 5. a) Schematic illustrating the Fabrication Process of a $Ti_3C_2T_x$ MXene/rGO Hybrid Aerogel by GO-Assisted Hydrothermal Assembly, Directional Freezing, And Freeze-Drying, b) EMI-shielding performances of epoxy/MGA nanocomposites (a-b reproduced with permission from ref. [87], Copyright 2018, American Chemical Society). c) Synthesis Procedure of rGO-Fe_3O_4 , d) SE_A vs frequency (c-d reproduced with permission from ref. [88], Copyright 2019, American Chemical Society).

In addition to hybrid conductive particles, researchers are also exploring the use of self-assembly methods to introduce magnetic particles into the GF structure to achieve a wider shielding bandwidth. For instance, Prasad *et al*. reported the two-step hydrothermal synthesis of MoS_2-rGO composites with magnetic particle $CoFe_2O_4$ on the surface.[89] The introduction of magnetic particles and MoS_2 layer makes the material to form multiple interface structure and moderate impedance matching, which improves the material magnetic loss and the SE_A efficiency of the shield. In order to further explore the influence of magnetic particle hybridization on the EMIS performance of graphene composite foam, Sushmita *et al*. reported the preparation of ferromagnetic hybrid particles and paramagnetic hybrid particles composite graphene structure by self-assembly method,[88] as shown in **Figure 5c.** They found that in the ferromagnetic hybrid composite GF, magnetic particles were the main factor affecting the EMIS performance of the composite material, while in the paramagnetic hybrid composite GF, the dielectric loss had an important effect on the composite material. In addition, it is further proved that materials with only high conductivity or permeability may not have better shielding performance, but it is particularly important to select nanoparticles with stronger dissipation to improve the EMIS performance of materials, as shown in Figure 5d.

4.2. Templated Synthesis of EMIS Materials

The templated synthesis refers to the preparation of composite hybrid foam by using foam material as the template and using physical and chemical methods to deposit graphene sheets and hybrid particles on the surface of the template. As one of the main methods to prepare graphene foam, template method has been widely studied by scientists because of its controllable structure, uniform distribution of graphene and controllable deposition thickness. The preparation of graphene and its derivatives foam by template method is mainly divided into metal template,[77] and organic template.[90]

4.2.1. Metal Template Synthesis

The metal formwork method, mainly use Ni foam with 3D network structure as the template, is the most widely used way in the template method. The organic gas is decomposed at high temperature. Graphene and its derivatives were deposited on the surface of the skeleton structure to obtain the GF structure under the catalysis of Ni,[91] and the preparation principle is

shown in **Figure 6a.**[92] This method has the advantages of controllable number of layers, easy preparation of large size, and high- quality graphene. Therefore, the prepared GF has higher conductivity, larger specific surface area, and structural adjustment, and therefore shows amazing performance in EMIS field.

At present, nickel and copper are mainly used as templates in the preparation of GF by CVD. Chen *et al*. developed a scheme to prepare GF with nickel foam as the substrate.[93] They first selected nickel foam, a 3D interconnected porous structure, as the matrix material for the growth template of GF. The nickel foam was surface treated to remove impurities and placed in a reactor at an ambient temperature of 1000 ℃. A gaseous mixture of CH4 and Ar were pumped into the reactor to introduce carbon sources. CH_4 was decomposed at high temperature, and the graphene sheet was deposited on the surface of nickel foam to form G-nickel composite foam. The composite foam was immersed in a hot HCl solution or $FeCl_3$ solution, then the metal nickel was removed to form GF. The GF obtained by this method has a high porosity of up to 99.7% and an ultra-low density of ~ 5 mg/cm^3. Compared with the self-assembly method, the GF prepared by CVD method has lower boundary resistance, and the movement of electrons in the sheet is almost unimpeded, thus improving the overall electrical conductivity of the material because the graphene prepared by CVD method does not introduce oxygen-containing functional groups and has fewer defects. The graphene 3D network structure has an amazing electrical conductivity up to ~10 s cm^{-1}, and its conductive properties are improved by 6 orders of magnitude compared with the GF prepared by graphene chemical derivatives.

In order to obtain larger synthetic size and more uniform spatial structure, the preparation process has been further simplified to improve the toughness of the composite GFs.[94] Compared with conventional preparation methods, the one-step process eliminates the impregnation process of polymethyl methacrylate (PMMA), while the graphene-nickel composite foam directly impregnates polydimethylsiloxane (PDMS). This preparation method can not only simplify the preparation process and save time, but also reduce the damage to the graphene sheet during the preparation process and ensure the integrity of the 3D network structure of graphene. The GF prepared by this method has extremely high EMIS efficiency. In the band of 30 MHz-1.5 GHz, the shielding efficiency of the shielding body exceeds 30 dB (1 mm thickness), and in the X band, the EMIS efficiency of the GF structure also reaches 20 dB.

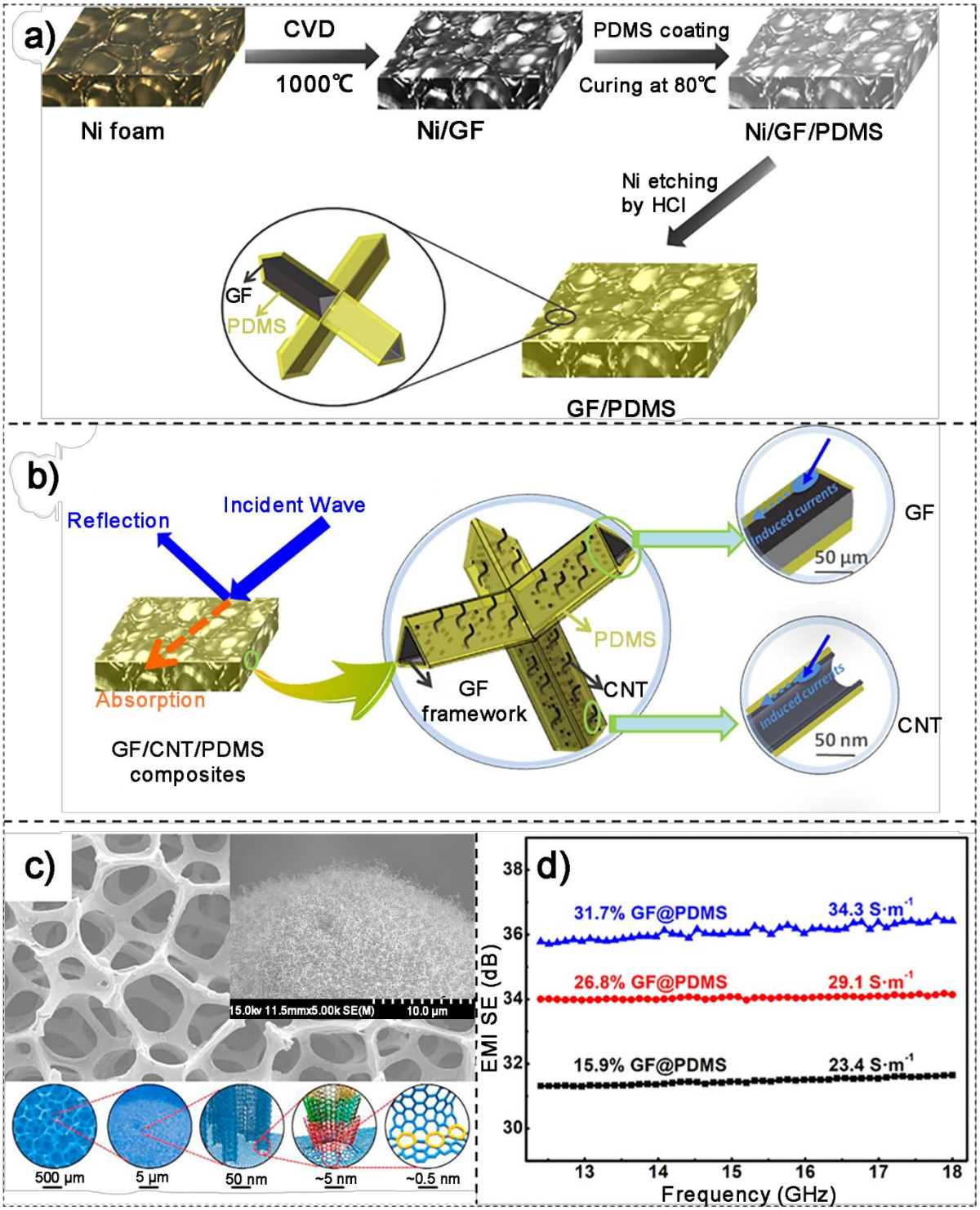

Figure 6. a) Schematic of GF/ polydimethylsiloxane (PDMS) composite fabrication process. b) Schematic illustration of effective EMIS by GF/CNT/PDMS hybrid composites through reflection and absorption (a-b reproduced with permission from ref. [92], Copyright 2016, Elsevier). c) Design strategy describing the control at multiple scales of structural design, and interface

reinforced strategy. (c reproduced with permission from ref. [95], Copyright 2017, Elsevier). d) EMIS effectiveness of the as-prepared GF@PDMS with three different GF contents and electrical conductivities in the frequencies ranging from 12.4 to 18 GHz (d reproduced with permission from ref.[96], Copyright 2018, American Chemical Society).

In order to further obtain GF materials with higher EMIS efficiency, Sun *et al*. prepared GF/CNT/PDMS composite foam materials by CVD method.[92] They reported the effect of CNT content on the shielding of composite materials and investigated the EMIS mechanism of multiphase composite materials. The addition of CNT increased the reflection performance of the material to some extent. However, due to the fact that the interconnect network structure has not changed substantially, the SE_R of the material does not enhance significantly with the increase of the content of CNT, when the content of graphene CNTs reaches a certain level. In the composite foam, the CNT embedded in the polymer enhanced the mutual disturbance between the shield and the electromagnetic wave and increased the energy dissipation of the electromagnetic wave, as shown in **Figure 6b.** In another study, Kong *et al*. reported the preparation of carbon nanowires/graphene composite foam material with excellent EMIS performance by uniformly growing carbon nanowires on graphene lining plate through covalent bonds, and the design structure was shown in **Figure 6c**.[95] The defects of carbon nanowires, and the polarization and electromagnetic attenuation enhanced by the interface between carbon nanowires and graphene make the material body have excellent electromagnetic wave absorption loss. In the 8-12 GHz band, the SE_A efficiency of carbon nanowires/graphene composite foam is close to 25 dB (1.6 mm thickness), and the overall EMIS exceeds 35 dB. After that, Li *et al*. further improved the template method and proposed the template guided annealing method. This method control GF density through the concentration of polyacrylonitrile (PAN) in the dimethylformamide (DMF) solvent, and successfully prepared a high-density GF of 27.2~69.2 mg/cm^3. Thanks to the relatively high density of GF, template removal can be accomplished without the protective layer covering the GF surface.[96] In addition, the GF prepared by this method can form a long-range interconnected network structure, as shown in **Figure 6d**, so that the material has a high SE_A efficiency. The EMIS efficiency of the material reached 36.1 dB (4.5 mm thickness) in the range of 8.2 -18 GHz.

4.2.2. Organic Template Synthesis

Scientists have invested a great deal of energy in the research of metal template method, and the graphene 3D mesh structure with better performance can be obtained.[97] However, the metal template method still has outstanding problems, such as the etching of templates.[95] Because of the high density of the metal template, the metal template needs to be etched to reduce the overall density of the material. During the etching process of the metal template, the original graphene sheet and its interconnect network fabric would be threatened, thus affecting the final properties of the material. Organic template method is to prepare graphene and its derivatives three-dimensional network structure through carbonization and deposition using organic foam structure as template.[98] Because the solvent of organic template etching is relatively mild and some templates have little effect on the density of materials, it can be avoided by etching. Therefore, the organic template method can reduce the damage to the original structure during the etching process and simplify the preparation process of foam structure.

For instance, Song *et al*. explored and successfully prepared CNT/graphene composite shell core foam structure without metal catalysis.[97] They chose SiO_2 nanowires as a template on which CNT can grow to form foams at 1100 ℃. CNT-GEP (graphene edge plane) composite foam was prepared by capturing carbon source at 800 ℃, and the preparation process was shown in **Figure 7a.** The CNT-GEP composite foam has an obvious shell-core structure. This unique structure has a higher density of defects, so that the material dielectric relaxation, tunnelling and interface effects can be changed, thus enhancing the EMIS efficiency of the material body. In the x-band, the EMIS efficiency of the material is close to 50 dB (3.6 mm thickness), as shown in **Figure 7b**.

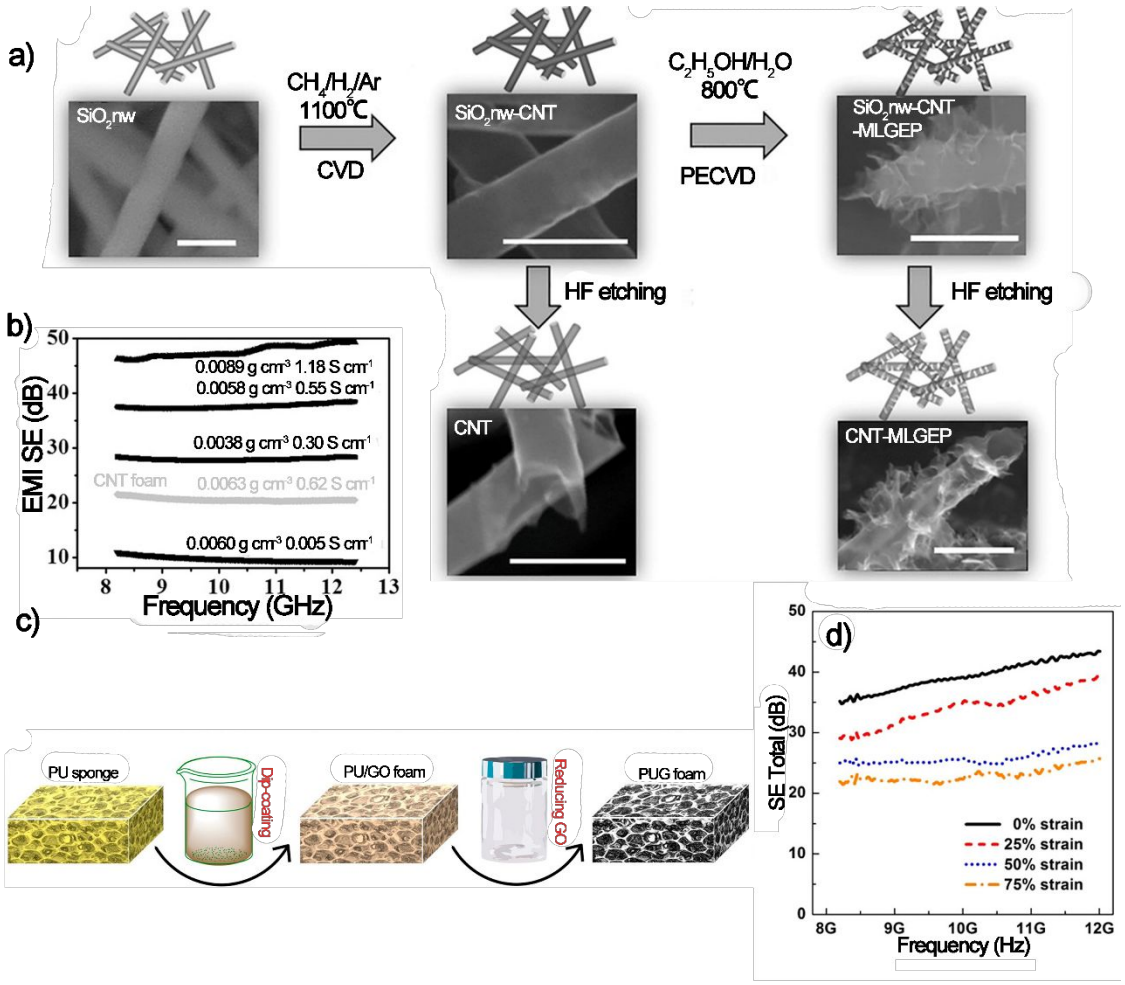

Figure 7. a) schematic of the fabrication of the CNT–MLGEP core–shell hybrid foam (scale bars: 500 nm), b) EMI SE in the X-band of the CNT/MLGEP foams with various densities-conductivities and the CNT foam (a-b reproduced with permission from ref. [97], Copyright 2017, Wiley). c) Overall fabrication process of the PUG foams, including dip-coating GO sheets onto the PU frameworks and then hydrothermally reducing by hydrazine vapor, d) SE total of the PUG-10 foam with a thickness of ~6 cm under different compressive strains (c-d reproduced with permission from ref. [99], Copyright 2016, American Chemical Society).

Pitkanenden *et al*. reported the preparation of CNT/carbon nanofiber composites using melamine foam as template through carbonization and CVD.[100] After carbonization, the melamine foam formed a 3D interconnect network carbon skeleton structure, and the CNTs were evenly distributed on the carbon nano-skeleton structure. CNTs grown on the surface of the skeleton play a crucial role in the absorption of electromagnetic waves, especially at low frequency. The long-range continuous interconnect network improves the microwave absorption

loss efficiency of materials at high frequency. The synergistic effect between CNT and continuous carbon fibre improves the absorption performance of the material, making the absorption loss efficiency of electromagnetic wave reach 30 dB (5 mm thickness) and effective absorption bandwidth reaching 18-26.5 GHz and providing a solution for future 5G electromagnetic shielding.

Yang *et al*. deposited the Co-based metal−organic framework (ZIF-67) on the melamine foam and carbonized it in a nitrogen atmosphere to obtain a three-dimensional microtubular structure with hierarchical carbon. Then, CNTs were grown on the surface of the microtubules to produce an ultralight three-dimensional network with metal Co encapsulated in the tip of the CNTs.[90] Under the support of this special structure, the Co/CNT/CS composite material has obtained excellent conductivity and satisfactory magnetic loss performance. It is worth noting that this composite material has extremely high matching impedance and multiple polarization, which gives the material high electromagnetic shielding absorption loss performance. This team investigated the effects of different reaction temperatures and times on the material's microwave absorption loss efficiency. They found that the morphology and composition of the material could be controlled by changing the reaction time and temperature, and further control the electromagnetic shielding efficiency of the material. Wu *et al*. investigated the preparation of a hierarchical carbon/rGO/FeO_x (CGF) composite by continuous impregnation and carbonization.[98] They impregnated melamine foam in a mixture of iron salts and GO produce a melamine/GO/FeO_x composite foam. During the impregnation process, GO was deposited on the 3D interconnect mesh framework of the melamine foam, while ferrite particles were modified on the foam structure. The composite foam was then carbonized at high temperature in an argon atmosphere to obtain a CGF composite. On the one hand, the carbonized melamine foam formed a N-doped carbon foam structure, and a large number of N atoms generated dipole polarization,. In addition, the layered carbon structure and the large internal cavity induce multiple microwave reflections, which significantly improved the absorption loss efficiency of the composite.

In another case, Shen *et al*. explored the use of cold templates to prepare graphene composite foams.[99] In this method, the polyurethane (PU) sponge is immersed in the GO suspension, and then the PU foam impregnated with GO is dried. Finally, rGO/PU composite foam can be obtained by chemical reduction of GO, as shown in **Figure 7c.** This method can also obtain a more regular 3D graphene network structure. Since graphene is coated on the outer layer

of the PU skeleton, a shell-core structure of graphene-PU is formed. Electromagnetic wave enters the graphene tube structure through the shell and is reflected by the graphene tube wall, which increases the material's absorption shielding efficiency and makes the material's EMIS efficiency reach over 35 dB (60 mm thickness) as shown in Figure 7d.

4.3. Sol-Gel Synthesis of GFs

The sol-gel method is commonly used to prepare polymer hydrogels or aerogels. In recent years, due to its relatively simple preparation process, the mild reaction conditions have been gradually developed and applied to the preparation of graphene-based composite foams. In this method, graphite oxide and other hybrid particles are dispersed uniformly in the water phase. A reducing agent such as ascorbic acid and hydrazine hydrate was added to the suspension. GO forms GO hydrogel under the action of reducing agents. The hydrogel was then freeze-dried and further treated to produce graphene aerogel,[101] as shown in **Figure 8a.**

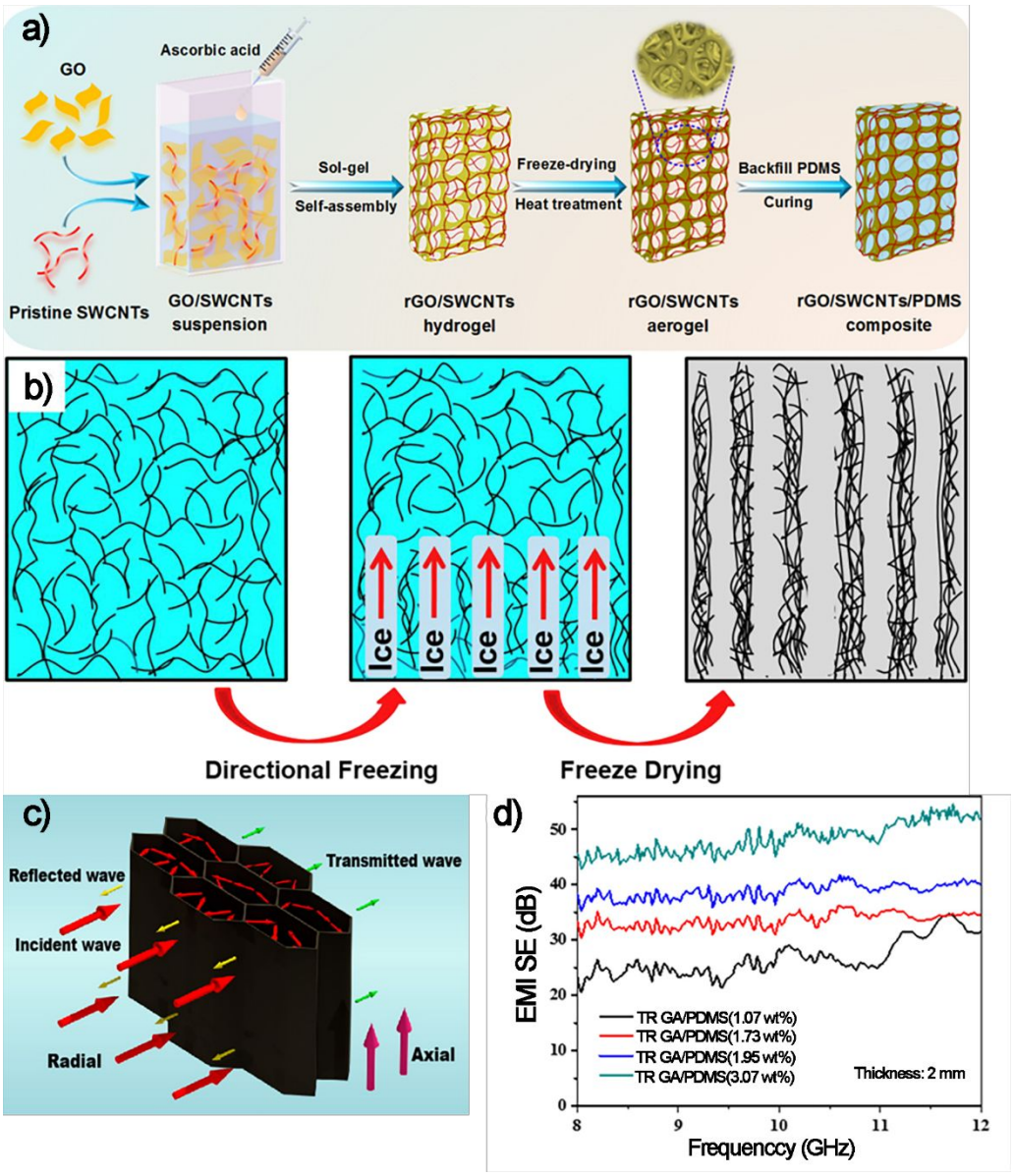

Figure 8. a) Schematic illustration of the fabrication procedure of PTGCA composites (a reproduced with permission from ref. [101], Copyright 2018, American Chemical Society). b) A schematic illustrating the directional-freezing and freeze-drying(b reproduced with permission from ref. [102] , Copyright 2016, Elsevier). c) Schematic illustrating the EMIS mechanisms for anisotropic epoxy/graphene composites along radial and axial directions(c reproduced with permission from ref. [103], Copyright 2016, American Chemical Society). d) Plots of EMIS effect vs frequency for TRGA/PDMS nanocomposites with different TRGA content with specimen thickness of 2 mm in the range of 8−12 GHz(d reproduced with permission from ref. [104], Copyright 2018, American Chemical Society)

Recently, Liu *et al*. prepared highly ordered and anisotropic porous GF structure by the sol-gel method combined with directional freeze-drying technology.[102] The preparation principle and structure are shown in **Figure 8b.** However, it is disappointing that the mechanical strength of the GF prepared by this method is not good enough to meet the requirements of practical application. Li *et al*. introduced this directional freeze-drying method for preparing highly structured GFs into the field of EMIS.[103] Firstly, the prepared graphene suspension was heat-treated to prepare graphene hydrogel. Secondly, the intermediate phase solid was obtained by directional freezing under the action of liquid nitrogen. Finally, the intermediate phase solid was freeze-dried to obtain the highly oriented anisotropic GF structure. Due to the special structure of material anisotropy, the material's conductivity in the axial direction was up to 980 s/m, but in the radial direction, it was only 96 s/m.

Similarly, due to the vertical and radial arrangement of a large number of graphene laminates, the SE_M and attenuation of electromagnetic wave incident in the radial direction were greatly increased. As shown in **Figure 8c**., the EMIS efficiency along the radial direction reaches 32 dB (4 mm). The team tried to add epoxy resin to the GF structure. The epoxy resin in the hole can effectively support the GF body, and the epoxy resin attached to the surface of the graphene hole can prevent the graphene from falling off, thereby achieving the material's mechanical strength. Xu *et al*. reported a two-step preparation of GF/PDMS composite foam.[104] The GF was prepared by the sol-gel method, and then PDMS was directly infiltrated into the GF by vacuum technology to prepare composite foams with high flexibility and EMIS performance. The tensile modulus of the composite material reached 11.73 MPa, far exceeding the pure PDMS tensile modulus. At 3.07 wt%, the electrical conductivity of the material was as high as 103 s/m. At the same content, the electrical conductivity of the composite foam was higher than that of the pure GF. At a graphene content of 3%, the EMIS efficiency of the composite foam reached 54dB (2 mm thickness), as shown in **Figure 8d**.

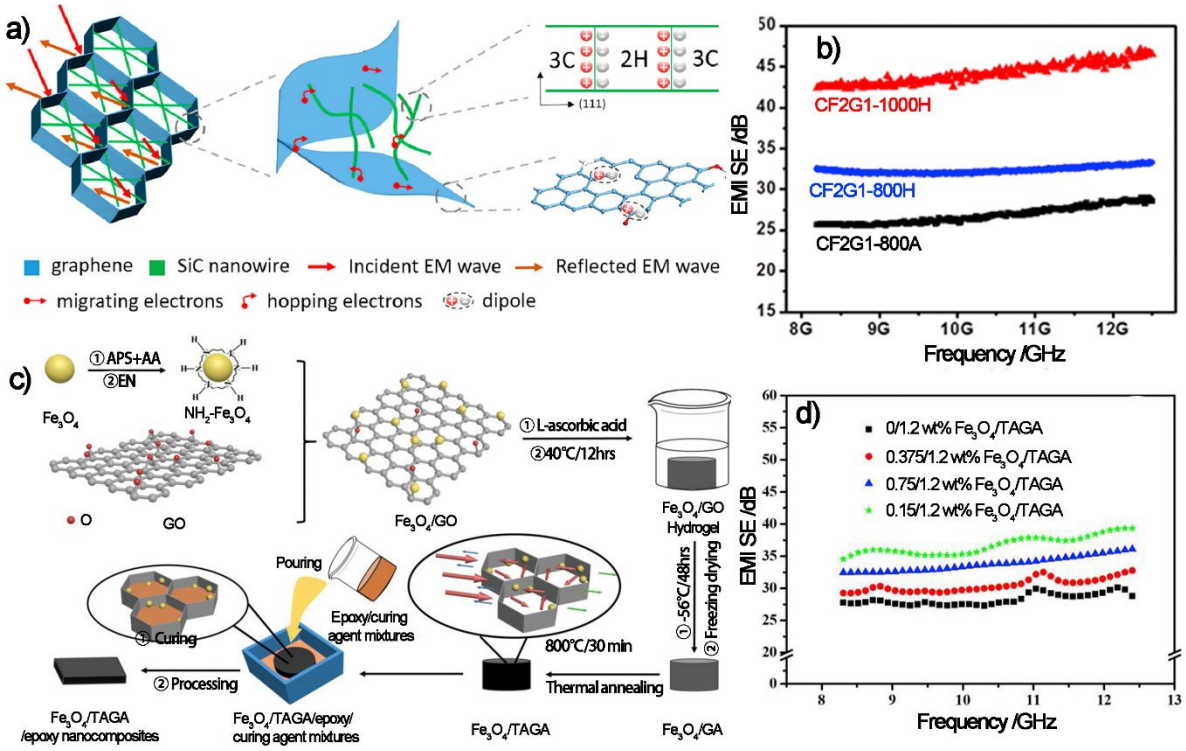

Figure 9. a)Schematic for the EM-wave absorption mechanisms of rGO/SiC nanowire foam composites (reproduced with permission from ref. [105], Copyright 2017, American Chemical Society). b) EMI shielding performance of CF2G1 aerogel (5 mm) with different treated conditions in the frequency range from 8.2 to 18 GHz(b reproduced with permission from ref. [106], Copyright 2017, Elsevier) c)Schematic diagram of the fabrication for the Fe_3O_4/TAGA/epoxy nanocomposites, d) EMI SE values of the Fe_3O_4/TAGA/epoxy nanocomposites (c-d reproduced with permission from ref. [107], Copyright 2019, Elsevier)

In order to further enhance the mechanical strength of GF prepared by the sol-gel method, Han *et al*. modified the sol-gel method by embedding silicon carbide nanowires into the graphene network structure to prepare the rGO/SiC-nanowire foam. The SiC nanowires embedded in the graphene mesh structure support the GF structure and improve the mechanical strength of the foam structure.[105] When the mass ratio of SiC nanowires was more than 30%, the dielectric constant and the EMIS performance of the created material increased with the increase of SiC content. The higher specific surface area of graphene and SiC nanowires increases charge accumulation, leading to stronger electron polarization. In addition, the twinned crystal interface of nanomaterials and a large number of folds can effectively enhance the electromagnetic losses

of composites, as shown in **Figure 9a.** In another study, Wan *et al*. reported the preparation of cellulose fiber (CF)/graphene composite nanomaterials by the sol-gel method.[106] With the support of CF, the structure of GF still has high mechanical properties after annealing. In addition, a larger conductive network was constructed between the carbonized CF and graphene sheets to further improve the electrical conductivity of CF/GF structure. The EMIS efficiency of the composite foam was over 40 dB with 5 mm thickness in X-band, as shown in **Figure 9b**. The team found that increasing the annealing temperature could improve the reduction degree of GO to some extent, and at the same time, it could give the foam structure super-high compression properties.

It is difficult for a single graphene composite polymer to achieve satisfactory EMIS performance in a wide band. Huangfu *et al*. grafted the modified Fe_3O_4 onto GO sheets and prepared dispersion solution.[107] Fe_3O_4/graphene composite foam was fabricated by sol-gel method. Finally, the epoxy resin is impregnated to the surface of the composite foam, as shown in **Figure 9c.** Magnetic particles can effectively increase the electromagnetic loss of the shielding body, which can greatly enhance the performance of GF in the low-frequency band and increase the EMIS bandwidth of the material. The EMIS efficiency of Fe_3O_4/ graphene/epoxy composite foam reaches 35 dB (3 mm thickness) in the X-band range, as shown in **Figure 9d**. In addition, Chen *et al*.[108] and Shen *et al*.[109] prepared Fe_3O_4/rGO/polystyrene (PS) and rGO@Fe_3O_4/polyetherimide composites, respectively, which both exceeded satisfied EMIS performance.

4.4. Other Methods for the Synthesis of GFs for EMIS

In addition to the above methods, researchers have developed steam/thermal stripping, foaming, steam induced phase separation and template etching approaches. With the development of preparation methods, the EMIS performance and mechanical strength of the prepared materials have been improved.

The steam/thermal stripping method utilizes hot steam generated during the reduction process to peel off graphene sheets to form GF. Niu *et al*. started off with a suspension of GO and obtained the GO membrane by vacuum filtration.[110] The GO film was floated on the surface of hydrazine hydrate in an airtight container and heated to 90 °C for 10 h to produce GF of 0.03 g/cm^3. During the reduction of GO by hydrazine hydrate steam, the oxygen-containing functional

groups of GO detach as CO, CO_2 and H_2O. During the separation of oxygen-containing functional groups, the graphene flakes were detached to form GF. This method can control the foaming ratio of GF by changing the amount of hydrazine hydrate. Yang *et al*. further explored the influence of heating rates on GF and the effect of bubble hole structure on EMIS effectiveness of materials.[111] It was found that the bubble structure greatly improved the absorption of electromagnetic wave energy by the GF, and the EMIS efficiency of the GF in the 8-60 GHz band reached 25 dB (2 mm).

The foaming method is often used to prepare various foam structures. This method has been applied successfully to prepare graphene-based EMIS materials. This preparation process is relatively simple, and the pore structure is uniform, so it has been recognized by scholars all over the world. Foaming methods include chemical foaming and physical foaming. The chemical foaming method usually incorporates a chemical foaming agent such as sodium hydrogen carbonate, ammonium carbonate, azobisisobutyronitrile (AIBN) or the like in advance in the polymer/graphene system. The chemical blowing agent generates gases under heating, hot pressing or the like, or the raw materials react with each other to release gases, so that the volume of the composite material is rapidly expanded to achieve rapid foaming of the material. Physical foaming methods usually use CO_2 or N_2 and other "green foaming agents", do not involve some toxic organic solvents and complex chemical reactions. Therefore, it is more environmentally friendly than the chemical foaming method.

Eswaraiah *et al*. successfully prepared a polyvinylidene fluoride (PVDF)/graphene composite foam by means of preparing a GF by a chemical foaming method[112]. The foaming agent is decomposed by hot pressing to prepare foam material. The PVDF/graphene composite foam EMIS material has an aperture size of 0.5 to 2 microns and shielding efficiency of about 28 dB in X-band at 7 wt.% graphene content, which is suitable for general commercial application. Gavgani *et al*. reported the preparation of graphene/polyurethane composite foam with high elastic modulus and high regularity by chemical foaming method,[113] as shown in **Figure 10a.** The prepared graphene composite foam has a conductivity of about 4.04 s m^{-1} and excellent EMIS performance. In the 8-12 GHz band. The EMIS ability of the designed material has reached to 23dB, and the specific EMIS efficiency was up to ~253 dB ($g^{-1}cm^{-3}$), as shown in **Figure 10b**. In another case, Zhang *et al*. successfully prepared PMMA/graphene composite microporous foam by using subcritical CO_2, an environmentally friendly foaming agent, as the foaming agent.[114]

The foams composite prepared by this method not only has uniform pore diameter and high porosity, but also has electromagnetic shielding efficiency over 13 dB in the 8-12 GHz band.

Water-vapour induced phase separation involves coating a mixture of polyetherimide/graphene/DMF casting solution on a glass substrate and then placing it in moist air. Since the DMF in the membrane is compatible with H_2O, a large amount of water vapor is absorbed from the air, which causes the DMF to continuously separate from the blend, leaving a porous structure, and the polymer/graphene composite is obtained. Recently, Li *et al*. reported the preparation of multilayer graphene composite foam structures with concentration gradient by water-vapour induced phase separation,[115] as shown in **Figure 10c.**The prepared graphene composite structure has a long-range interconnection network structure. They explored that the optimized gradient structure can make the sandwich structure capture more electromagnetic wave energy and cause electromagnetic wave attenuation to achieve the improvement of the material's absorption performance. The EMIS efficiency of the composite materials in the range of 12-18 GHz exceeds 25 dB as shown in **Figure 10d**.

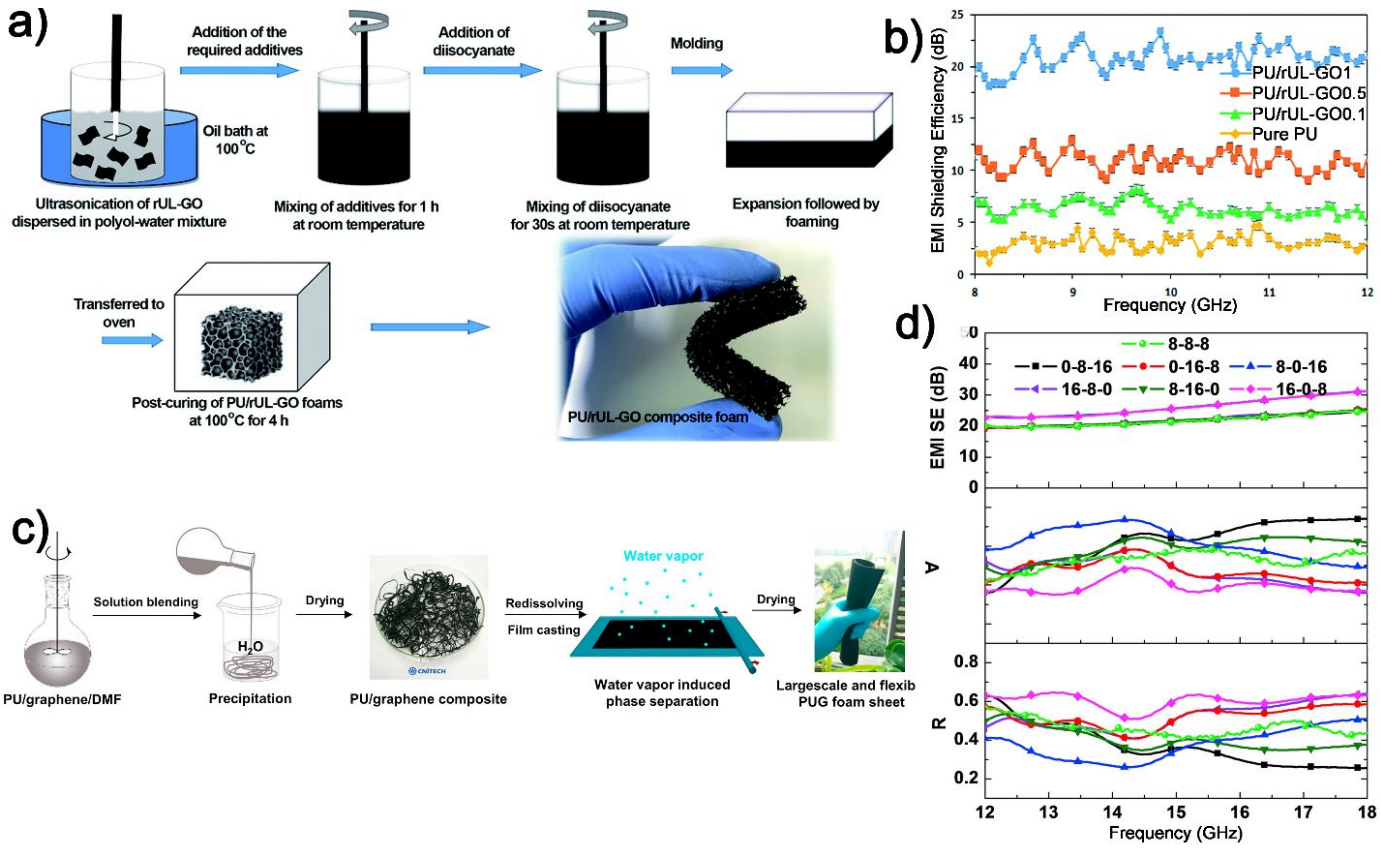

Figure 10. Preparation steps of PU/rUL-GO composite foam, b) EMI shielding efficiency of PU/rUL/GO composite foam at different frequencies (a-b reproduced with permission from ref. [116], Copyright 2016, Royal Society of Chemistry). c) Schematic illustration for the preparation of PUG foams, d) SE total, A and R of PUG foams in Ku-band: 0-8-16, 16-8-0, 0-16-8, 8-16-0, 8-0-16, 16-0-8 and 8-8-8 (the control). (c-d reproduced with permission from ref. [115], Copyright 2017, Elsevier).

Template etching involves mixing easily removed materials into the polymer/graphene mixture as fillers. After the blend is formed, the fillers are chemically separated from the original structure, leaving a porous structure. Yan *et al*. prepared PS composite foam with graphene content up to 30 wt% by using the mould-press-etching method.[117] In this method, PS resin was firstly mixed with graphene in solution, and then the composite was mechanically blended with $CaCO_3$ particles for hot-pressing forming. Finally, the $CaCO_3$ particles in the obtained PS/graphene/$CaCO_3$ composite material were etched with dilute hydrochloric acid to obtain PS/ graphene composite foam. The pore size of the composite foam is determined by the size of $CaCO_3$ particles. The density or foaming ratio can be adjusted by adjusting the amount of $CaCO_3$ mixed in PS/ graphene. The average EMIS performance of PS composite foam with a thickness of 2.5 mm and a graphene content of 30 wt.% at X-band is ~17 dB (0.27 g/cm^3) and ~29 dB (0.45g/cm^3), which can meet the requirements of EMIS materials. Recently, Wang *et al*. obtained PVDF/PS/CNT composites by melt blending, and after molding them, the PS components were etched away by xylene. finally, a PVDF composite foam with a CNT content of 15 wt% was obtained (0.79 g/cm^3).[118] In the X-band, the average EMIS efficiency of the composite foam reaches 56.72 dB, which is beyond the use requirements of EMIS materials.

In summary, we can find that: the 3D graphene structure, on one hand, gives full play to the unique properties of graphene such as high conductivity and ultra-low density, endowing the material with considerable electromagnetic shielding efficiency. On the other hand, this 3D structure realizes a longer-range conductive network, increases the conductivity of the material, and the bubble structure in the 3D structure also forms more interfaces, further improving the EMIS efficiency of graphene materials. By combining graphene with other reinforcing materials to prepare graphene composite foam, the mechanical strength of graphene foam can be improved and the application scenarios of graphene foam can be expanded. By comparison, it can be found

that the composition, preparation process, and treatment method are different, and the electromagnetic shielding efficiency of 3D graphene materials also changes to different degrees, as shown in Table 2.

Table 2. Summary of preparation methods, components and shielding effectiveness of 3d graphene

Preparation Methods	Component	Annealing (℃)	Thickness (mm)	EMIS Efficiency	Ref.
Self-assembly	rGO	600	2	-34 dB	84
	MWCNT/rGO	400	2	-39 dB	80
	Epoxy/P-GA	1300	2	35 dB	86
	MXene/rGO	-	2	56.4 dB	87
	MoS_2-rGO/$CoFe_2O_4$	-	1.4	19.26 dB	89
Template Synthesis	CNT/rGO/PDMS	-	2	75 dB	92
	G/PDMS	-	1	30 dB	94
	CNWs/G	600	1.6	36 dB	95
	GF@PDMS	-	4.5	36.1 dB	96
	CNT/ MLGEP	-	3.6	66 dB	97
	C/rGO/FeOx	-	2.1	−51.2 dB	98
	PU/G	-	60	57 dB	99
	CNT/CNF	770	5	30 dB	100
Sol-gel	PDMS/rGO/SWCNT	-	2	31 dB	101
	G/epoxy	1300	4	32 dB	103
	rGO/PDMS	-	2	56 dB	104
	CF/RGO	1000	5	47.8 dB	106
	Fe_3O_4/TAGA/epoxy	800	3	35 dB	107
	PS/ TGO/Fe_3O_4	-	-	30 dB	108
	PEI/graphene@Fe_3O_4	-	2.5	18.2 dB	109
Others	f-G/PVDF	-	-	20 dB	112
	PU/ rUL-GO	-	2.5	23 dB	116

G/PMMA	-	2.4	19 dB	[114]

5. Conclusion and outlooks

In summary, starting from the EMIS mechanism, we demonstrated the EMIS theory of the microstructure of graphene and the macroscopic structure of GF, systematically analyzed the methods for controlling the 3D network structure and mechanical strength of GFs in different preparation methods. Based on the above case studies, it can be found that GF-based EMIS materials could fully exert the good electrical conductivity and mechanical properties of graphene to achieve higher EMIS effectiveness. Magnetic particle hybrid GF EMIS materials can make up for the insufficient performance of single graphene material in low frequency band. By adjusting the 3D structure and hybridization of graphene, the lightweight, broadband, and highly efficient GF-based EMIS materials can be obtained, which can meet the requirements of electromagnetic shielding in future electronic development.

In future studies, there is still great space for the development of graphene-based EMIS materials. In addition, studies on the preparation of ternary or multi-component hybrid GF EMIS materials is still in the initial stage. The synergistic effect of multiple hybrid particles and the SE_A mechanism of multicomponent composite materials need to be further studied. On the other hand, it is also necessary to access a controlled method for preparing GF structure by a large number of experiments to obtain GF structures with high porosity, uniform pore size, and longer continuity. Finally, the large-scale industrial production of graphene will promote wide applications of graphene-based EMIS materials.

Author Information

Corresponding Authors

Zhiqiang Su- State Key Laboratory of Chemical Resource Engineering, Beijing University of Chemical Technology, 100029 Beijing, China. E-mail: suzq@mail.buct.edu.cn.

Gang Wei- College of Chemistry and Chemical Engineering, Qingdao University, 266071 Qingdao, China. E-mail: weigroup@qdu.edu.cn.

Fucheng Wang-Zhejiang University of Technology, Hangzhou, China. E-mail: fcwang@ziliref.com

Author Contributions

‡These authors contributed equally.

Acknowledgments

The authors gratefully acknowledge the financial support from the National Natural Science Foundation of China (NSFC, Grant no. 51873016, 51873225). M. Zhang acknowledges the support and funding from China Scholarship Council (CSC).

Conflicts of Interest

There are no conflicts to declare.

References

(1) Zhang, Q.; Liang, Q.; Zhang, Z.; Kang, Z.; Liao, Q.; Ding, Y.; Ma, M.; Gao, F.; Zhao, X.; Zhang, Y., Electromagnetic Shielding Hybrid Nanogenerator For Health Monitoring and Protection. *Adv. Funct. Mater.* **2018,** *28* (1), 1703801.
(2) Zhang, X.; Wei, W.; Zhang, S.; Wen, B.; Su, Z., Advanced 3D Nanohybrid Foam Based on Graphene Oxide: Facile Fabrication Strategy, Interfacial Synergetic Mechanism, and Excellent Photocatalytic Performance. *Sci. China Mater.* **2019,** *62* (12), 1888-1897.
(3) Chen, J.; Zhao, D.; Ge, H.; Wang, J., Graphene Oxide-Deposited Carbon Fiber/Cement Composites for Electromagnetic Interference Shielding Application. *Constr. Build. Mater.* **2015,** *84*, 66-72.
(4) Jia, L.-C.; Yan, D.-X.; Liu, X.; Ma, R.; Wu, H.-Y.; Li, Z.-M., Highly Efficient and Reliable Transparent Electromagnetic Interference Shielding Film. *ACS Appl. Mater. Interfaces* **2018,** *10* (14), 11941-11949.
(5) Song, W.-L.; Guan, X.-T.; Fan, L.-Z.; Cao, W.-Q.; Wang, C.-Y.; Zhao, Q.-L.; Cao, M.-S., Magnetic and Conductive Graphene Papers Toward Thin Layers of Effective Electromagnetic Shielding. *J. Mater. Chem. A* **2015,** *3* (5), 2097-2107.
(6) Song, W.-L.; Guan, X.-T.; Fan, L.-Z.; Cao, W.-Q.; Wang, C.-Y.; Cao, M.-S., Tuning Three-Dimensional Textures with Graphene Aerogels for Ultra-Light Flexible Graphene/Texture Composites of Effective Electromagnetic Shielding. *Carbon* **2015,** *93*, 151-160.

(7) Zeng, Z.; Jin, H.; Chen, M.; Li, W.; Zhou, L.; Zhang, Z., Lightweight and Anisotropic Porous MWCNT/WPU Composites for Ultrahigh Performance Electromagnetic Interference Shielding. *Adv. Funct. Mater.* **2016,** *26* (2), 303-310.
(8) Zhang, X.; Liu, W.; Wang, H.; Zhao, X.; Zhang, Z.; Nienhaus, G. U.; Shang, L.; Su, Z., Self-assembled Thermosensitive Iuminescent Nanoparticles with Peptide-Au Conjugates for Cellular Imaging and Drug Delivery. *Chin. Chem. Lett.* **2019,** *10* (1016), 1016.
(9) Zhao, B.; Zhao, C.; Li, R.; Hamidinejad, S. M.; Park, C. B., Flexible, Ultrathin, and High-efficiency Electromagnetic Shielding Properties of Poly (Vinylidene Fluoride)/Carbon Composite Films. *ACS Appl. Mater. Interfaces* **2017,** *9* (24), 20873-20884.
(10) Chen, Y.; Zhang, H. B.; Yang, Y.; Wang, M.; Cao, A.; Yu, Z. Z., High-Performance Epoxy Nanocomposites Reinforced With Three-Dimensional Carbon Nanotube Sponge For Electromagnetic Interference Shielding. *Adv. Funct. Mater.* **2016,** *26* (3), 447-455.
(11) Zaszczynska, A.; Sajkiewicz, P.; Gradys, A., Piezoelectric Scaffolds as Smart Materials for Neural Tissue Engineering. *Polymers* **2020,** *12* (1), 161.
(12) Kheifets, L.; Afifi, A. A.; Shimkhada, R., Public Health Impact of Extremely Low-Frequency Electromagnetic Fields. *Environ. Health Perspect.* **2006,** *114* (10), 1532-1537.
(13) Wang, X.-X.; Ma, T.; Shu, J.-C.; Cao, M.-S., Confinedly Tailoring Fe_3O_4 Clusters-NG to Tune Electromagnetic Parameters and Microwave Absorption with Broadened Bandwidth. *Chem. Eng. J.* **2018,** *332*, 321-330.
(14) Hashemi, S.; Abdolali, A., Room Shielding with Frequency-Selective Surfaces for Electromagnetic Health Application. *Int J Microw Wirel T* **2017,** *9* (2), 291-298.
(15) Joshi, A.; Bajaj, A.; Singh, R.; Anand, A.; Alegaonkar, P.; Datar, S., Processing of Graphene Nanoribbon Based Hybrid Composite for Electromagnetic Shielding. *Composites Part B* **2015,** *69*, 472-477.
(16) Li, X.-H.; Li, X.; Liao, K.-N.; Min, P.; Liu, T.; Dasari, A.; Yu, Z.-Z., Thermally Annealed Anisotropic Graphene Aerogels and Their Electrically Conductive Epoxy Composites with Excellent Electromagnetic Interference Shielding Efficiencies. *ACS Appl. Mater. Interfaces* **2016,** *8* (48), 33230-33239.
(17) Dong, S.; Shi, Q.; Huang, W.; Jiang, L.; Cai, Y., Flexible Reduced Graphene Oxide Paper with Excellent Electromagnetic Interference Shielding for Terahertz Wave. *J. Mater. Sci. Mater. Electron.* **2018,** *29* (20), 17245-17253.
(18) Liu, T.; Guo, Y.; Zhang, Z.; Miao, Z.; Zhang, X.; Su, Z., Fabrication of Hollow CuO/PANI Hybrid Nanofibers for Non-enzymatic Electrochemical Detection of H_2O_2 and Glucose. *Sens. Actuators, B* **2019,** *286*, 370-376.
(19) Xu, S. T.; Fan, F.; Cheng, J.; Chen, H.; Ma, W.; Huang, Y.; Chang, S., Active Terahertz Shielding and Absorption Based on Graphene Foam Modulated by Electric and Optical Field Excitation. *Adv. Opt. Mater.* **2019,** *7* (18), 1900555.
(20) D'Aloia, A. G.; D'Amore, M.; Sarto, M. S., Terahertz Shielding Effectiveness of Graphene-based Multilayer Screens Controlled by Electric Field Bias in a Reverberating Environment. *IEEE Trans. Terahertz Sci. Technol.* **2015,** *5* (4), 628-636.
(21) Liu, L.; Das, A.; Megaridis, C. M., Terahertz Shielding of Carbon Nanomaterials and Their Composites—a Review and Applications. *Carbon* **2014,** *69*, 1-16.
(22) Chen, H.; Ma, W.; Huang, Z.; Zhang, Y.; Huang, Y.; Chen, Y., Graphene-based Materials toward Microwave and Terahertz Absorbing Stealth Technologies. *Adv. Opt. Mater.* **2019,** *7* (8), 1801318.

(23) Choi, Y.-S.; Yoo, Y.-H.; Kim, J.-G.; Kim, S.-H., A Comparison of the Corrosion Resistance of Cu-Ni-Stainless Steel Multilayers Used for EMI Shielding. *Surf. Coat. Technol.* **2006,** *201* (6), 3775-3782.
(24) Gelves, G. A.; Al-Saleh, M. H.; Sundararaj, U., Highly Electrically Conductive and High-performance EMI Shielding Nanowire/Polymer Nanocomposites by Miscible Mixing and Precipitation. *J. Mater. Chem.* **2011,** *21* (3), 829-836.
(25) Sahoo, P.; Aepuru, R.; Panda, H. S.; Bahadur, D., Ice-templated Synthesis of Multifunctional Three Dimensional Graphene/Noble Metal Nanocomposites and Their Mechanical, Electrical, Catalytic, and Electromagnetic Shielding Properties. *Sci. Rep.* **2015,** *5*, 17726.
(26) Šafářová, V.; Militký, J., Multifunctional Metal Composite Textile Shields Against Electromagnetic Radiation—Effect of Various Parameters on Electromagnetic Shielding Effectiveness. *Polym. Compos.* **2017,** *38* (2), 309-323.
(27) Frackowiak, S.; Ludwiczak, J.; Leluk, K.; Orzechowski, K.; Kozlowski, M., Foamed Poly(Lactic Acid) Composites with Carbonaceous Fillers for Electromagnetic Shielding. *Mater. Des.* **2015,** *65*, 749-756.
(28) Zhang, K.; Yu, H.-O.; Yu, K.-X.; Gao, Y.; Wang, M.; Li, J.; Guo, S., A Facile Approach to Constructing Efficiently Segregated Conductive Networks in Poly(Lactic Acid)/Silver Nanocomposites Via Silver Plating on Microfibers for Electromagnetic Interference Shielding. *Compos. Sci. Technol.* **2018,** *156*, 136-143.
(29) Zakiyan, S. E.; Azizi, H.; Ghasemi, I., Influence of Chain Mobility on Rheological, Dielectric and Electromagnetic Interference Shielding Properties of Poly Methyl-Methacrylate Composites Filled with Graphene and Carbon Nanotube. *Compos. Sci. Technol.* **2017,** *142*, 10-19.
(30) Zhao, B.; Park, C. B., Tunable Electromagnetic Shielding Properties of Conductive Poly (Vinylidene Fluoride)/Ni Chain Composite Films with Negative Permittivity. *J. Mater. Chem. C* **2017,** *5* (28), 6954-6961.
(31) Zhang, K.; Li, G.-H.; Feng, L.-M.; Wang, N.; Guo, J.; Sun, K.; Yu, K.-X.; Zeng, J.-B.; Li, T.; Guo, Z., Ultralow Percolation Threshold and Enhanced Electromagnetic Interference Shielding in Poly(L-Lactide)/Multi-Walled Carbon Nanotube Nanocomposites with Electrically Conductive Segregated Networks. *J. Mater. Chem. C* **2017,** *5* (36), 9359-9369.
(32) Zhang, M.; Li, Y.; Su, Z.; Wei, G., Recent Advances in The Synthesis and Applications of Graphene–Polymer Nanocomposites. *Polym. Chem.* **2015,** *6* (34), 6107-6124.
(33) Wu, J.; Chen, J.; Zhao, Y.; Liu, W.; Zhang, W., Effect of Electrophoretic Condition on The Electromagnetic Interference Shielding Performance of Reduced Graphene Oxide-Carbon Fiber/Epoxy Resin Composites. *Composites Part B* **2016,** *105*, 167-175.
(34) Liu, W.; Zhang, X.; Wei, G.; Su, Z., Reduced Graphene Oxide-based Double Network Polymeric Hydrogels for Pressure and Temperature Sensing. *Sensors* **2018,** *18* (9), 3162.
(35) Yu, X.; Sun, S.; Zhou, L.; Miao, Z.; Zhang, X.; Su, Z.; Wei, G., Removing Metal Ions from Water with Graphene–bovine Serum Albumin Hybrid Membrane. *Nanomaterials* **2019,** *9* (2), 276.
(36) Cao, M.-S.; Wang, X.-X.; Cao, W.-Q.; Yuan, J., Ultrathin Graphene: Electrical Properties and Highly Efficient Electromagnetic Interference Shielding. *J. Mater. Chem. C* **2015,** *3* (26), 6589-6599.
(37) Tang, X.; Zhou, H.; Cai, Z.; Cheng, D.; He, P.; Xie, P.; Zhang, D.; Fan, T., Generalized 3D Printing of Graphene-Based Mixed-Dimensional Hybrid Aerogels. *ACS nano* **2018,** *12* (4), 3502-3511.

(38) Rao, B. B.; Yadav, P.; Aepuru, R.; Panda, H.; Ogale, S.; Kale, S., Single-Layer Graphene-Assembled 3D Porous Carbon Composites with PVA And Fe_3O_4 Nano-Fillers: An Interface-Mediated Superior Dielectric and EMI Shielding Performance. *Phys. Chem. Chem. Phys.* **2015,** *17* (28), 18353-18363.
(39) Ding, X.; Huang, Y.; Li, S.; Zhang, N.; Wang, J., 3D Architecture Reduced Graphene Oxide-Mos_2 Composite: Preparation and Excellent Electromagnetic Wave Absorption Performance. *Composites Part A* **2016,** *90*, 424-432.
(40) Li, J.-S.; Huang, H.; Zhou, Y.-J.; Zhang, C.-Y.; Li, Z.-T., Research Progress of Graphene-based Microwave Absorbing Materials in The Last Decade. *J. Mater. Res.* **2017,** *32* (7), 1213-1230.
(41) Schelkunoff, S. A., On Diffraction and Radiation of Electromagnetic Waves. *Phys. Rev.* **1939,** *56* (4), 308.
(42) Munalli, D.; Dimitrakis, G.; Chronopoulos, D.; Greedy, S.; Long, A., Electromagnetic Shielding Effectiveness of Carbon Fibre Reinforced Composites. *Composites Part B* **2019,** *173*, 106906.
(43) YAMAGUCHI, D.; TAKEUCHI, K.; HAYASHI, M., Circuit Simulator for Prediction of Electromagnetic Induction up to Data Transmission Frequency in Railway Environment. *Q. Rep.* **2016,** *57* (4), 287-292.
(44) Schulz, R. B.; Plantz, V.; Brush, D., Shielding Theory and Practice. *IEEE Trans. Electromagn. Compat.* **1988,** *30* (3), 187-201.
(45) Ghosh, S.; Ganguly, S.; Remanan, S.; Mondal, S.; Jana, S.; Maji, P. K.; Singha, N.; Das, N. C., Ultra-light Weight, Water Durable and Flexible Highly Electrical Conductive Polyurethane Foam for Superior Electromagnetic Interference Shielding Materials. *J. Mater. Sci. Mater. Electron.* **2018,** *29* (12), 10177-10189.
(46) Yang, K.; Mei, H.; Han, D.; Cheng, L., Enhanced Electromagnetic Shielding Property of C/Sic Composites Via Electrophoretically-deposited Cnts Onto Sic Coating. *Ceram. Int.* **2018,** *44* (16), 20187-20191.
(47) Han, J.; Wang, X.; Qiu, Y.; Zhu, J.; Hu, P., Infrared-transparent Films Based on Conductive Graphene Network Fabrics for Electromagnetic Shielding. *Carbon* **2015,** *87*, 206-214.
(48) Tong, X. C., Advanced Materials and Design for Electromagnetic Interference Shielding. *CRC press:* 2016.
(49) Farukh, M.; Singh, A. P.; Dhawan, S., Enhanced Electromagnetic Shielding Behavior of Multi-walled Carbon Nanotube Entrenched Poly (3, 4-Ethylenedioxythiophene) Nanocomposites. *Compos. Sci. Technol.* **2015,** *114*, 94-102.
(50) Benhamou, S. M.; Hamouni, M.; Khaldi, S., Theoretical Approach of Electromagnetic Shielding of Multilayer Conductive Sheets. *Prog. Electromagn. Res.* **2015,** *41*, 167-175.
(51) Guo, T.; Chen, X.; Su, L.; Li, C.; Huang, X.; Tang, X.-Z., Stretched Graphene Nanosheets Formed The "Obstacle Walls" In Melamine Sponge Towards Effective Electromagnetic Interference Shielding Applications. *Mater. Des.* **2019,** *182*, 108029.
(52) Sharif, F.; Arjmand, M.; Moud, A. A.; Sundararaj, U.; Roberts, E. P., Segregated Hybrid Poly (Methyl Methacrylate)/Graphene/Magnetite Nanocomposites for Electromagnetic Interference Shielding. *ACS Appl. Mater. Interfaces* **2017,** *9* (16), 14171-14179.
(53) Xu, W.; Wang, G.-S.; Yin, P.-G., Designed Fabrication of Reduced Graphene Oxides/Ni Hybrids for Effective Electromagnetic Absorption and Shielding. *Carbon* **2018,** *139*, 759-767.

(54) Shen, B.; Li, Y.; Yi, D.; Zhai, W.; Wei, X.; Zheng, W., Strong Flexible Polymer/Graphene Composite Films With 3D Saw-Tooth Folding for Enhanced and Tunable Electromagnetic Shielding. *Carbon* **2017,** *113*, 55-62.
(55) Ma, L.; Lu, Z.; Tan, J.; Liu, J.; Ding, X.; Black, N.; Li, T.; Gallop, J.; Hao, L., Transparent Conducting Graphene Hybrid Films to Improve Electromagnetic Interference (EMI) Shielding Performance of Graphene. *ACS Appl. Mater. Interfaces* **2017,** *9* (39), 34221-34229.
(56) Wang, J.; Ouyang, Z.; Ren, Z.; Li, J.; Zhang, P.; Wei, G.; Su, Z., Self-assembled Peptide Nanofibers on Graphene Oxide as a Novel Nanohybrid For Biomimetic Mineralization of Hydroxyapatite. *Carbon* **2015,** *89*, 20-30.
(57) Zhao, X.; Zhang, P.; Chen, Y.; Su, Z.; Wei, G., Recent Advances in The Fabrication and Structure-Specific Applications of Graphene-based Inorganic Hybrid Membranes. *Nanoscale* **2015,** *7* (12), 5080-5093.
(58) Li, K.; Zhang, Z.; Li, D.; Zhang, W.; Yu, X.; Liu, W.; Gong, C.; Wei, G.; Su, Z., Biomimetic Ultralight, Highly Porous, Shape-adjustable, and Biocompatible 3D Graphene Minerals via Incorporation of Self-assembled Peptide Nanosheets. *Adv. Funct. Mater.* **2018,** *28* (29), 1801056.
(59) Ando, T., The Electronic Properties of Graphene and Carbon Nanotubes. *NPG Asia Mater.* **2009,** *1* (1), 17.
(60) Zhang, X.; Wei, W.; Zhang, S.; Wen, B.; Su, Z., Advanced 3D Nanohybrid Foam Based on Graphene Oxide: Facile Fabrication Strategy, Interfacial Synergetic Mechanism, and Excellent Photocatalytic Performance. *Sci. China Mater.* **2019,** *9* (2199-4501), 88-97.
(61) Miao, Z.; Shi, J.; Liu, T.; Li, P.; Su, Z.; Wei, G., Adamantane-Modified Graphene Oxide for Cyanate Ester Resin Composites with Improved Properties. *Appl. Sci.* **2019,** *9* (5), 881.
(62) Al-Ghamdi, A. A.; Al-Ghamdi, A. A.; Al-Turki, Y.; Yakuphanoglu, F.; El-Tantawy, F., Electromagnetic Shielding Properties of Graphene/Acrylonitrile Butadiene Rubber Nanocomposites for Portable and Flexible Electronic Devices. *Composites Part B* **2016,** *88*, 212-219.
(63) Song, H.; Zhang, X.; Liu, Y.; Su, Z., Developing Graphene-based Nanohybrids for Electrochemical Sensing. *Chem.Rec.* **2019,** *19* (2-3), 534-549.
(64) Liu, W.; Zhang, X.; Zhou, L.; Shang, L.; Su, Z., Reduced Graphene Oxide (rGO) Hybridized Hydrogel as a Near-infrared (NIR)/pH Dual-responsive Platform for Combined Chemo-photothermal Therapy. *J. Colloid Interface Sci.* **2019,** *536*, 160-170.
(65) He, J.-Z.; Wang, X.-X.; Zhang, Y.-L.; Cao, M.-S., Small Magnetic Nanoparticles Decorating Reduced Graphene Oxides to Tune the Electromagnetic Attenuation Capacity. *J. Mater. Chem. C* **2016,** *4* (29), 7130-7140.
(66) Wang, K.; Chen, Y.; Li, H.; Chen, B.; Zeng, K.; Chen, Y.; Chen, H.; Liu, Q.; Liu, H., Fe/N-codoped Hollow Carbonaceous Nanospheres Anchored on Reduced Graphene Oxide for Microwave Absorption. *ACS Appl. Nano Mater.* **2019,** *2*, 8063-8074.
(67) Wu, Y.; Wang, Z.; Liu, X.; Shen, X.; Zheng, Q.; Xue, Q.; Kim, J.-K., Ultralight Graphene Foam/Conductive Polymer Composites for Exceptional Electromagnetic Interference Shielding. *ACS Appl. Mater. Interfaces* **2017,** *9* (10), 9059-9069.
(68) Gedler, G.; Antunes, M.; Velasco, J.; Ozisik, R., Electromagnetic shielding effectiveness of polycarbonate/graphene nanocomposite foams processed in 2-steps with supercritical carbon dioxide. *Mater. Lett.* **2015,** *160*, 41-44.
(69) Dragoman, M.; Ghimpu, L.; Obreja, C.; Dinescu, A.; Plesco, I.; Dragoman, D.; Braniste, T.; Tiginyanu, I., Ultra-Lightweight Pressure Sensor Based on Graphene Aerogel Decorated with Piezoelectric Nanocrystalline Films. *Nanotechnol.* **2016,** *27* (47), 475203.

(70) Wang, Z.; Shen, X.; Akbari Garakani, M.; Lin, X.; Wu, Y.; Liu, X.; Sun, X.; Kim, J.-K., Graphene Aerogel/Epoxy Composites with Exceptional Anisotropic Structure and Properties. *ACS Appl. Mater. Interfaces* **2015,** *7* (9), 5538-5549.
(71) Lin, Y.; Hou, G.; Su, X.; Bi, S.; Tang, J. In *Compressible Ni and Reduced Graphene Oxide (Ni-rGO) Coated Polymer Foams for Electromagnetic Interference (EMI) Shielding.*, Earth Environ. Sci., IOP Publishing: 2018; p 012031.
(72) Lu, D.; Mo, Z.; Liang, B.; Yang, L.; He, Z.; Zhu, H.; Tang, Z.; Gui, X., Flexible, Lightweight Carbon Nanotube Sponges and Composites for High-Performance Electromagnetic Interference Shielding. *Carbon* **2018,** *133*, 457-463.
(73) WENG, L.; MIN, Y., New Research Progress of Electromagnetic Shielding and Absorbing Composites Based on Graphene. *J.Funct. Mater.* **2017,** (12), 8.
(74) Li, Y.; Pei, X.; Shen, B.; Zhai, W.; Zhang, L.; Zheng, W., Polyimide/Graphene Composite Foam Sheets with Ultrahigh Thermostability For Electromagnetic Interference Shielding. *RSC Adv.* **2015,** *5* (31), 24342-24351.
(75) Li, D.; Zhang, W.; Yu, X.; Wang, Z.; Su, Z.; Wei, G., When Biomolecules Meet Graphene: From Molecular Level Interactions to Material Design and Applications. *Nanoscale* **2016,** *8* (47), 19491-19509.
(76) Zhang, P.; Zhang, X.; Zhang, S.; Lu, X.; Li, Q.; Su, Z.; Wei, G., One-Pot Green Synthesis, Characterizations, and Biosensor Application of Self-Assembled Reduced Graphene Oxide–Gold Nanoparticle Hybrid Membranes. *J. Mater. Chem. B* **2013,** *1* (47), 6525-6531.
(77) Wu, Y.; Wang, Z.; Liu, X.; Shen, X.; Zheng, Q.; Xue, Q.; Kim, J. K., Ultralight Graphene Foam/Conductive Polymer Composites for Exceptional Electromagnetic Interference Shielding. *ACS Appl Mater Interfaces* **2017,** *9* (10), 9059-9069.
(78) Liang, C.; Qiu, H.; Han, Y.; Gu, H.; Song, P.; Wang, L.; Kong, J.; Cao, D.; Gu, J., Superior Electromagnetic Interference Shielding 3D Graphene Nanoplatelets/Reduced Graphene Oxide Foam/Epoxy Nanocomposites with High Thermal Conductivity. *J. Mater. Chem. C* **2019,** *7* (9), 2725-2733.
(79) Liu, P.; Zhang, Y.; Yan, J.; Huang, Y.; Xia, L.; Guang, Z., Synthesis of Lightweight N-Doped Graphene Foams with Open Reticular Structure for High-Efficiency Electromagnetic Wave Absorption. *Chem. Eng. J.* **2019,** *368*, 285-298.
(80) Chen, H.; Huang, Z.; Huang, Y.; Zhang, Y.; Ge, Z.; Qin, B.; Liu, Z.; Shi, Q.; Xiao, P.; Yang, Y.; Zhang, T.; Chen, Y., Synergistically Assembled MWCNT/Graphene Foam with Highly Efficient Microwave Absorption in Both C and X Bands. *Carbon* **2017,** *124*, 506-514.
(81) Xu, Y.; Sheng, K.; Li, C.; Shi, G., Self-Assembled Graphene Hydrogel Via a One-Step Hydrothermal Process. *ACS nano* **2010,** *4* (7), 4324-4330.
(82) Wu, Y.; Yi, N.; Huang, L.; Zhang, T.; Fang, S.; Chang, H.; Li, N.; Oh, J.; Lee, J. A.; Kozlov, M.; Chipara, A. C.; Terrones, H.; Xiao, P.; Long, G.; Huang, Y.; Zhang, F.; Zhang, L.; Lepro, X.; Haines, C.; Lima, M. D.; Lopez, N. P.; Rajukumar, L. P.; Elias, A. L.; Feng, S.; Kim, S. J.; Narayanan, N. T.; Ajayan, P. M.; Terrones, M.; Aliev, A.; Chu, P.; Zhang, Z.; Baughman, R. H.; Chen, Y., Three-Dimensionally Bonded Spongy Graphene Material with Super Compressive Elasticity and Near-Zero Poisson's Ratio. *Nat Commun* **2015,** *6*, 6141.
(83) Shen, B.; Li, Y.; Yi, D.; Zhai, W.; Wei, X.; Zheng, W., Microcellular Graphene Foam for Improved Broadband Electromagnetic Interference Shielding. *Carbon* **2016,** *102*, 154-160.
(84) Zhang, Y.; Huang, Y.; Chen, H.; Huang, Z.; Yang, Y.; Xiao, P.; Zhou, Y.; Chen, Y., Composition and Structure Control of Ultralight Graphene Foam for High-Performance Microwave Absorption. *Carbon* **2016,** *105*, 438-447.

(85) Gonzalez, M.; Baselga, J.; Pozuelo, J., Modulating the Electromagnetic Shielding Mechanisms by Thermal Treatment of High Porosity Graphene Aerogels. *Carbon* **2019,** *147*, 27-34.
(86) Chen, Y.; Zhang, H.-B.; Wang, M.; Qian, X.; Dasari, A.; Yu, Z.-Z., Phenolic Resin-Enhanced Three-Dimensional Graphene Aerogels and Their Epoxy Nanocomposites with High Mechanical and Electromagnetic Interference Shielding Performances. *Compos. Sci. Technol.* **2017,** *152*, 254-262.
(87) Zhao, S.; Zhang, H. B.; Luo, J. Q.; Wang, Q. W.; Xu, B.; Hong, S.; Yu, Z. Z., Highly Electrically Conductive Three-Dimensional $Ti_3C_2T_x$ MXene/Reduced Graphene Oxide Hybrid Aerogels with Excellent Electromagnetic Interference Shielding Performances. *ACS Nano* **2018,** *12* (11), 11193-11202.
(88) Sushmita, K.; Menon, A. V.; Sharma, S.; Abhyankar, A. C.; Madras, G.; Bose, S., Mechanistic Insight into the Nature of Dopants in Graphene Derivatives Influencing Electromagnetic Interference Shielding Properties in Hybrid Polymer Nanocomposites. *J.Physic.Chem.C* **2019,** *123* (4), 2579-2590.
(89) Prasad, J.; Singh, A. K.; Haldar, K. K.; Tomar, M.; Gupta, V.; Singh, K., $CoFe_2O_4$ Nanoparticles Decorated MoS_2-reduced Graphene Oxide Nanocomposite for Improved Microwave Absorption and Shielding Performance. *RSC Adv.* **2019,** *9* (38), 21881-21892.
(90) Yang, N.; Luo, Z. X.; Zhu, G. R.; Chen, S. C.; Wang, X. L.; Wu, G.; Wang, Y. Z., Ultralight Three-Dimensional Hierarchical Cobalt Nanocrystals/N-Doped CNTs/Carbon Sponge Composites with a Hollow Skeleton toward Superior Microwave Absorption. *ACS Appl Mater Interfaces* **2019,** *11* (39), 35987-35998.
(91) Sun, X.; Liu, X.; Shen, X.; Wu, Y.; Wang, Z.; Kim, J.-K., Reprint of Graphene Foam/Carbon nanotube/Poly(dimethyl siloxane) Composites for Exceptional Microwave Shielding. *Composites Part A* **2017,** *92*, 190-197.
(92) Sun, X.; Liu, X.; Shen, X.; Wu, Y.; Wang, Z.; Kim, J.-K., Graphene Foam/Carbon Nanotube/Poly (Dimethyl Siloxane) Composites for Exceptional Microwave Shielding. *Composites Part A* **2016,** *85*, 199-206.
(93) Chen, Z.; Ren, W.; Gao, L.; Liu, B.; Pei, S.; Cheng, H.-M., Three-Dimensional Flexible and Conductive Interconnected Graphene Networks Grown by Chemical Vapour Deposition. *Nat. Mater.* **2011,** *10* (6), 424.
(94) Chen, Z.; Xu, C.; Ma, C.; Ren, W.; Cheng, H. M., Lightweight and Flexible Graphene Foam Composites for High-Performance Electromagnetic Interference Shielding. *Adv. Mater.* **2013,** *25* (9), 1296-1300.
(95) Kong, L.; Yin, X.; Han, M.; Yuan, X.; Hou, Z.; Ye, F.; Zhang, L.; Cheng, L.; Xu, Z.; Huang, J., Macroscopic Bioinspired Graphene Sponge Modified with In-Situ Grown Carbon Nanowires and Its Electromagnetic Properties. *Carbon* **2017,** *111*, 94-102.
(96) Li, H.; Jing, L.; Ngoh, Z. L.; Tay, R. Y.; Lin, J.; Wang, H.; Tsang, S. H.; Teo, E. H. T., Engineering of High-Density Thin-Layer Graphite Foam-Based Composite Architectures with Superior Compressibility and Excellent Electromagnetic Interference Shielding Performance. *ACS Appl Mater Interfaces* **2018,** *10* (48), 41707-41716.
(97) Song, Q.; Ye, F.; Yin, X.; Li, W.; Li, H.; Liu, Y.; Li, K.; Xie, K.; Li, X.; Fu, Q.; Cheng, L.; Zhang, L.; Wei, B., Carbon Nanotube-Multilayered Graphene Edge Plane Core-Shell Hybrid Foams for Ultrahigh-Performance Electromagnetic-Interference Shielding. *Adv.Mater.Des.Inter.* **2017,** *29* (31), 1701583.

(98) Wu, Z.; Huang, T.; Li, T.; Li, L., Facile Preparation of a Hierarchical C/rGO/FeO_x Composite with Superior Microwave Absorption Performance. *Langmuir* **2019,** *35* (10), 3688-3693.
(99) Shen, B.; Li, Y.; Zhai, W.; Zheng, W., Compressible Graphene-Coated Polymer Foams with Ultralow Density for Adjustable Electromagnetic Interference (EMI) Shielding. *ACS Appl Mater Interfaces* **2016,** *8* (12), 8050-7.
(100) Pitkanen, O.; Tolvanen, J.; Szenti, I.; Kukovecz, A.; Hannu, J.; Jantunen, H.; Kordas, K., Lightweight Hierarchical Carbon Nanocomposites with Highly Efficient and Tunable Electromagnetic Interference Shielding Properties. *ACS Appl Mater Interfaces* **2019,** *11* (21), 19331-19338.
(101) Zhao, S.; Yan, Y.; Gao, A.; Zhao, S.; Cui, J.; Zhang, G., Flexible Polydimethylsilane Nanocomposites Enhanced with a Three-Dimensional Graphene/Carbon Nanotube Bicontinuous Framework for High-Performance Electromagnetic Interference Shielding. *ACS Appl Mater Interfaces* **2018,** *10* (31), 26723-26732.
(102) Liu, T.; Huang, M.; Li, X.; Wang, C.; Gui, C.-X.; Yu, Z.-Z., Highly Compressible Anisotropic Graphene Aerogels Fabricated by Directional Freezing for Efficient Absorption of Organic Liquids. *Carbon* **2016,** *100*, 456-464.
(103) Li, X. H.; Li, X.; Liao, K. N.; Min, P.; Liu, T.; Dasari, A.; Yu, Z. Z., Thermally Annealed Anisotropic Graphene Aerogels and Their Electrically Conductive Epoxy Composites with Excellent Electromagnetic Interference Shielding Efficiencies. *ACS Appl Mater Interfaces* **2016,** *8* (48), 33230-33239.
(104) Xu, F.; Chen, R.; Lin, Z.; Qin, Y.; Yuan, Y.; Li, Y.; Zhao, X.; Yang, M.; Sun, X.; Wang, S.; Peng, Q.; Li, Y.; He, X., Superflexible Interconnected Graphene Network Nanocomposites for High-Performance Electromagnetic Interference Shielding. *ACS Omega* **2018,** *3* (3), 3599-3607.
(105) Han, M.; Yin, X.; Hou, Z.; Song, C.; Li, X.; Zhang, L.; Cheng, L., Flexible and Thermostable Graphene/SiC Nanowire Foam Composites with Tunable Electromagnetic Wave Absorption Properties. *ACS Appl Mater Interfaces* **2017,** *9* (13), 11803-11810.
(106) Wan, Y.-J.; Zhu, P.-L.; Yu, S.-H.; Sun, R.; Wong, C.-P.; Liao, W.-H., Ultralight, Super-Elastic and Volume-Preserving Cellulose Fiber/Graphene Aerogel for High-Performance Electromagnetic Interference Shielding. *Carbon* **2017,** *115*, 629-639.
(107) Huangfu, Y.; Liang, C.; Han, Y.; Qiu, H.; Song, P.; Wang, L.; Kong, J.; Gu, J., Fabrication and Investigation on The Fe_3O_4/Thermally Annealed Graphene Aerogel/Epoxy Electromagnetic Interference Shielding Nanocomposites. *Compos. Sci. Technol.* **2019,** *169*, 70-75.
(108) Chen, Y.; Wang, Y.; Zhang, H.-B.; Li, X.; Gui, C.-X.; Yu, Z.-Z., Enhanced Electromagnetic Interference Shielding Efficiency of Polystyrene/Graphene Composites with Magnetic Fe_3O_4 Nanoparticles. *Carbon* **2015,** *82*, 67-76.
(109) Shen, B.; Zhai, W.; Tao, M.; Ling, J.; Zheng, W., Lightweight, Multifunctional Polyetherimide/Graphene@Fe_3O_4 Composite Foams for Shielding of Electromagnetic Pollution. *ACS Appl Mater Interfaces* **2013,** *5* (21), 11383-91.
(110) Niu, Z.; Chen, J.; Hng, H. H.; Ma, J.; Chen, X., A Leavening Strategy to Prepare Reduced Graphene Oxide Foams. *Adv. Mater.* **2012,** *24* (30), 4144-4150.
(111) Yang, S. J.; Kang, J. H.; Jung, H.; Kim, T.; Park, C. R., Preparation of a Freestanding, Macroporous Reduced Graphene Oxide Film as An Efficient and Recyclable Sorbent for Oils and Organic Solvents. *J. Mater. Chem. A* **2013,** *1* (33), 9427-9432.

(112) Eswaraiah, V.; Sankaranarayanan, V.; Ramaprabhu, S., Functionalized Graphene–PVDF Foam Composites for EMI Shielding. *Macromol. Mater. Eng.* **2011,** *296* (10), 894-898.
(113) Gavgani, J. N.; Adelnia, H.; Zaarei, D.; Gudarzi, M. M., Lightweight Flexible Polyurethane/Reduced Ultra large Graphene Oxide Composite Foams for Electromagnetic Interference Shielding. *RSC Adv.* **2016,** *6* (33), 27517-27527.
(114) Zhang, H.-B.; Yan, Q.; Zheng, W.-G.; He, Z.; Yu, Z.-Z., Tough Graphene−Polymer Microcellular Foams for Electromagnetic Interference Shielding. *ACS Appl. Mater. Interfaces* **2011,** *3* (3), 918-924.
(115) Li, Y.; Shen, B.; Yi, D.; Zhang, L.; Zhai, W.; Wei, X.; Zheng, W., The Influence of Gradient and Sandwich Configurations on The Electromagnetic Interference Shielding Performance of Multilayered Thermoplastic Polyurethane/Graphene Composite Foams. *Compos. Sci. Technol.* **2017,** *138*, 209-216.
(116) Gavgani, J. N.; Adelnia, H.; Zaarei, D.; Moazzami Gudarzi, M., Lightweight Flexible Polyurethane/Reduced Ultra large Graphene Oxide Composite Foams for Electromagnetic Interference Shielding. *RSC Adv.* **2016,** *6* (33), 27517-27527.
(117) Yan, D.-X.; Ren, P.-G.; Pang, H.; Fu, Q.; Yang, M.-B.; Li, Z.-M., Efficient Electromagnetic Interference Shielding of Lightweight Graphene/Polystyrene Composite. *J. Mater. Chem.* **2012,** *22* (36), 18772-18774.
(118) Wang, H.; Zheng, K.; Zhang, X.; Ding, X.; Zhang, Z.; Bao, C.; Guo, L.; Chen, L.; Tian, X., 3D Network Porous Polymeric Composites with Outstanding Electromagnetic Interference Shielding. *Compos. Sci. Technol.* **2016,** *125*, 22-29.